Environ Monit Assess (2024) 196:1098
https://doi.org/10.1007/s10661-024-13172-2

RESEARCH

Examining the drivers of forest cover change and deforestation susceptibility in Northeast India using multicriteria decision-making models

Rajkumar Guria · Manoranjan Mishra · Biswaranjan Baraj · Shreerup Goswami · Celso Augusto Guimarães Santos · Richarde Marques da Silva · Karma Detsen Ongmu Bhutia

Received: 18 May 2024 / Accepted: 24 September 2024 / Published online: 24 October 2024
© The Author(s), under exclusive licence to Springer Nature Switzerland AG 2024

Abstract The increasing rates of forest cover change and heightened vulnerability to deforestation present significant environmental challenges in Northeast India. This study investigates the dynamics of forest cover change and susceptibility to deforestation in this region from 2001 to 2021, utilizing data from the Hansen Global Forest Change (HGFC) product on the Google Earth Engine (GEE) platform. A suite of multicriteria decision-making (MCDM) models—including *VlseKriterijumska optimizacija I Kompromisno Resenje* (VIKOR), Simple Additive Weighting (SAW), Evaluation Based on Distance from Average Solution (EDAS), and Weighted Aggregates Sum Product Assessment (WASPAS)—was employed to assess changes in forest cover and deforestation susceptibility across varied zones. Multicollinearity tests confirmed the relevance of the factors influencing deforestation. Statistical validations, such as the Wilcoxon Signed Ranks Test, underscored the models' robustness, revealing statistically significant outcomes. Additionally, Receiver Operating Characteristic (ROC) curve and Area Under the Curve (AUC) analysis demonstrated the superior fit of the VIKOR model (AUC = 0.938) compared to SAW (AUC = 0.901), EDAS (AUC = 0.895), and WASPAS (AUC = 0.864) in predicting current deforestation susceptibility. Validation affirmed the reliability of all MCDM methods, with VIKOR displaying high sensitivity (True Positive Rate, TPR = 0.878) and optimal AUC (0.938). Correlation analyses among the models identified significant inter-relationships, notably

R. Guria · M. Mishra · B. Baraj · K. D. O. Bhutia
Department of Geography, Fakir Mohan University, Vyasa Vihar, Nuapadhi, Balasore 756089, Odisha, India
e-mail: rkguria.007@gmail.com

M. Mishra
e-mail: geo.manu05@gmail.com

B. Baraj
e-mail: biswaranjan.baraj@gmail.com

K. D. O. Bhutia
e-mail: karmagcr14@gmail.com

S. Goswami
Department of Geology, Utkal University, Vani Vihar, Bhubaneswar 751004, Odisha, India
e-mail: goswamishreerup@gmail.com

C. A. G. Santos (✉)
Department of Civil and Environmental Engineering, Federal University of Paraíba, João Pessoa, Paraíba 58051-900, Brazil
e-mail: celso@ct.ufpb.br

R. M. da Silva
Department of Geosciences, Federal University of Paraíba, João Pessoa, Paraíba 58051-900, Brazil
e-mail: richarde@geociencias.ufpb.br

a positive correlation between EDAS and SAW, and a negative correlation between VIKOR and SAW. The regions of Assam, Nagaland, Mizoram, and Arunachal Pradesh were identified as experiencing significant forest cover loss, indicating a pronounced susceptibility to future deforestation. These findings underscore the need for immediate intervention to address this critical environmental issue.

Keywords Analytical Approaches · Google Earth Engine · Hansen Global Forest Change · Biodiversity threats · Developmental pressures · Explanatory factors

Introduction

In recent decades, deforestation and environmental degradation have emerged as pressing global concerns, with significant threats from climate change and human activities increasingly jeopardizing forest ecosystems and exacerbating environmental risks for ecosystems and human societies (Basu & Basu, 2023; Chen et al., 2024; Shah et al., 2024). Characterized by the Food and Agriculture Organization (2022) as a significant reduction in the quantity and quality of forest biological resources, deforestation has far-reaching consequences including reduced biodiversity, increased pollution, global warming, climate change, soil erosion, and disruption of the water cycle (Santos et al., 2021). With forests sequestering approximately 662 billion tonnes of carbon and contributing around USD 1.52 trillion to the global gross domestic product, supporting the livelihoods of about 33 million people worldwide, the last three decades (1990–2020) have seen around 420 million hectares deforested, predominantly in tropical regions (Mo et al., 2023). This makes identifying the causes of deforestation and areas susceptible to it crucial for formulating effective mitigation measures, afforestation strategies, and policies (Abugre & Sackey, 2022; Dagar et al., 2023; Forest Resources Assessment, 2020; Kumar et al., 2014; Kumari et al., 2019; Mishra & Francaviglia, 2021; Schug et al., 2023). Recognizing these challenges, this study introduces a novel approach by employing Multicriteria Decision-Making (MCDM) models to analyze the drivers of forest cover change and deforestation susceptibility in Northeast India—a region of ecological significance and considerable environmental challenges. The integration of MCDM in forest conservation, particularly in this complex and understudied region, represents an innovative stride toward a holistic understanding of deforestation impacts and the development of more effective conservation strategies.

While numerous studies have leveraged remote sensing datasets and geographical information systems to analyze deforestation and land degradation (Silva et al., 2023a, 2023b), traditional statistical tools like frequency ratio (FR), logistic regression (LR), random forest (RF), and fragmentation approach (FA) predominantly focus on quantifying deforestation susceptibility based on a mixture of physical and anthropogenic parameters (Zerouali et al., 2023). Although these methods have significantly advanced our understanding of the causal factors behind deforestation, they often do not capture the complex interplay of socio-economic, ecological, and climatic influences. To address these limitations, recent efforts have incorporated machine learning and deep learning techniques to enhance the probability assessment of deforestation susceptibility (Altarez et al., 2023; Saha et al., 2022). Building on these developments, this study introduces an innovative approach by employing diverse MCDM models to comprehensively assess the drivers of forest cover change and deforestation susceptibility in Northeast India. Unlike previous methodologies, MCDM allows for the systematic integration and analysis of a broad range of criteria, making it possible to develop a more nuanced understanding of the multifaceted influences on deforestation, particularly in a region as ecologically and socially complex as Northeast India.

The choice and comparative analysis of MCDM models are critical for optimizing decision outcomes in scenarios characterized by complex, often conflicting criteria. The selection of the most appropriate MCDM model hinges on factors including the nature of the decision problem, the diversity of criteria involved, and the data's availability and robustness. As noted by Hosseini et al. (2024), different MCDM models present distinct advantages regarding simplicity, accuracy, and their capacity to integrate both qualitative and quantitative data effectively. By systematically comparing these models, this study aims to identify the most suitable approach that not only enhances the robustness of the decision-making process but also aligns closely with the specific

conservation objectives and stakeholder needs in Northeast India. This methodological rigor ensures that our analysis remains sensitive to the regional complexities and the multifaceted nature of deforestation drivers, thereby contributing to more targeted and effective forest conservation strategies.

Currently, the integration of geospatial techniques with MCDM models represents a powerful tool for accurately identifying areas at risk of deforestation. This approach has been successfully applied in various studies, demonstrating its efficacy in pinpointing vulnerable regions (Bhutia et al., 2024; Saha et al., 2020, 2021; Sahana et al., 2018). MCDM models are particularly valuable in forest conservation contexts, where decisions must balance multiple, often competing criteria—such as ecological efficiency, economic cost, and sustainability. By facilitating a comprehensive analysis that considers these diverse factors, MCDM models enhance the decision-making process, enabling policymakers and conservationists to devise strategies that are not only effective but also equitable and sustainable. This study leverages these models to offer a nuanced assessment of deforestation risks in Northeast India, aiming to provide actionable insights that support both local and broader-scale forest conservation initiatives.

In 2015, global deforestation resulted in the loss of approximately 10 million hectares of forest, a devastating trend that continues to affect many countries, including India (Food and Agriculture Organization, 2024). In India, the pressures of agricultural expansion, rapid urbanization, and illegal logging exacerbate deforestation, leading to significant biodiversity loss and altering local and regional climates. Each year, about 1.5 million hectares of Indian forests are transformed into barren landscapes, representing approximately 1% of the nation's forested land (Sudhakar Reddy et al., 2016). Agriculture remains the dominant cause of worldwide deforestation, responsible for 80% of all deforestation, with construction and urban development accounting for 15% and 5%, respectively (Kayet et al., 2021). A particularly impactful agricultural practice in India is Jhum cultivation, or 'shifting cultivation', which is prevalent in the mountainous and forest-rich regions of Southeast Asia (Giri et al., 2020). This practice involves cyclical clearing of forests by cutting and burning vegetation to create temporarily fertile arable land, only to abandon it as soil fertility declines before repeating the process in new areas. Jhum cultivation encompasses about 86% of India's total cultivated area (Pandey et al., 2022) and presents considerable environmental challenges exacerbated by demographic pressures and the escalating demand for food (Paul et al., 2020). This backdrop of ongoing deforestation and its drivers underscores the urgency and necessity of implementing innovative, effective strategies such as those explored in our study using Geographic Information Systems (GIS) and MCDM methodologies.

According to the Forest Survey of India (2021), the first decade of the millennium witnessed severe degradation of tropical deciduous and evergreen forests in developing countries, especially in Southeast Asia, where logging and agriculture were the primary culprits. The dynamics of deforestation are complex, varying significantly across different regions and changing over time due to a blend of climatic, environmental, and anthropogenic factors. Influential climatic and environmental factors include rainfall patterns, temperature fluctuations, air pollution levels, drought occurrences, forest density, floods, and forest fires, while key physical factors encompass soil quality, geology, geomorphology, and proximity to water bodies. Anthropogenic influences such as population density, settlement expansion, and road infrastructure development also play critical roles (Da Silva et al., 2023a, 2023b). Among these, Jhum cultivation remains a predominant practice that continues to erode the region's dense forest cover, posing a substantial threat to its ecological health (Rawat et al., 2018). Given these multifaceted drivers and their regional specificities, there is a pressing need for employing advanced decision-making tools like MCDM models, integrated with GIS, to conduct a nuanced analysis that can inform more targeted and effective forest conservation strategies. This study leverages these sophisticated methodologies to dissect and understand the intricate patterns of deforestation susceptibility in Northeast India, aiming to contribute robust insights into forest management and conservation efforts.

While previous studies have shed light on various aspects of deforestation in Northeast India, they often lack comprehensive long-term analysis and rarely apply advanced technological approaches.

For instance, Babu (2014) provides valuable historical insights into deforestation during the colonial period in Nagaland. Nag (2022) examines how changes in rainfall patterns in Cherrapunji, linked to climate change, deforestation, and industrial activities, pose environmental and socio-economic challenges. Furthermore, Rawat et al. (2018) investigate the profound ecological impacts of population growth, Jhum cultivation, and urbanization on forest degradation in the region. Despite these valuable contributions, there remains a significant research gap in conducting detailed long-term analyses and effectively pinpointing areas susceptible to deforestation using state-of-the-art tools. This study aims to bridge this gap by employing GIS integrated with MCDM models to conduct an in-depth analysis of deforestation trends and dynamics in the relatively underexplored region of Northeast India. By leveraging these advanced technologies, this research provides a novel perspective and robust methodological framework that can greatly assist policymakers and conservation efforts in formulating strategies that are not only informed by historical data but are also predictive and preventative. This approach ensures a more sustainable management of forest resources and helps mitigate the risk of future deforestation effectively.

Understanding the complexities of deforestation requires a comprehensive analysis that encompasses both natural and human elements of ecosystems (Bax & Francesconi, 2018; Saha et al., 2020). In response, the objectives of this research are twofold: (1) to evaluate deforestation susceptibility maps in Northeast India by utilizing advanced GIS integrated with MCDM methodologies, and (2) to analyze changes in forest cover over the past two decades (2000 – 2020). Unlike previous methodologies that often rely on singular data sources or simpler analytical frameworks, our integrated use of GIS and MCDM models allows for a more holistic evaluation of deforestation dynamics. By combining diverse data sets and leveraging MCDM for decision analysis, this approach not only identifies but also quantifies the relative importance of various deforestation drivers, providing a clearer understanding of how multiple factors interact in complex environments. This methodological advancement enables more effective and targeted conservation strategies. Moreover, the inclusion of stakeholder input through participatory approaches ensures that the solutions developed are practical and grounded in local realities, further enhancing the applicability and sustainability of conservation efforts. This study introduces several novel aspects to the field of forest conservation:

1. Integration of MCDM: Although widely used across various disciplines, the application of MCDM in forest conservation, particularly in the context of Northeast India, is pioneering. This approach enables the unique amalgamation of ecological, socio-economic, and climatic data to assess deforestation susceptibility comprehensively.
2. Localized Study with Broad Implications: By focusing on Northeast India, a region of rich biodiversity and significant environmental challenges, this study contributes unique insights into the global understanding of deforestation dynamics, offering strategies that are applicable both locally and globally.
3. Comprehensive Data Analysis: Employing an array of data sources, including remote sensing, ground surveys, and government reports, integrated through MCDM, enhances the precision and applicability of our findings, providing a nuanced understanding of the drivers of deforestation.
4. Development of a Deforestation Susceptibility Index: This study also pioneers the development of a deforestation susceptibility index, tailored to the specific environmental and socio-economic characteristics of Northeast India, aimed at assisting policymakers and conservationists in prioritizing and strategizing interventions effectively.
5. Stakeholder Engagement: The incorporation of a participatory approach, involving local stakeholders in the criteria weighting process, ensures that the outcomes are deeply reflective of local realities and conservation priorities. Identifying areas susceptible to deforestation and analyzing historical trends are critical for informing effective forest management assessments and shaping policies that mitigate deforestation impacts while promoting sustainable land use practices.

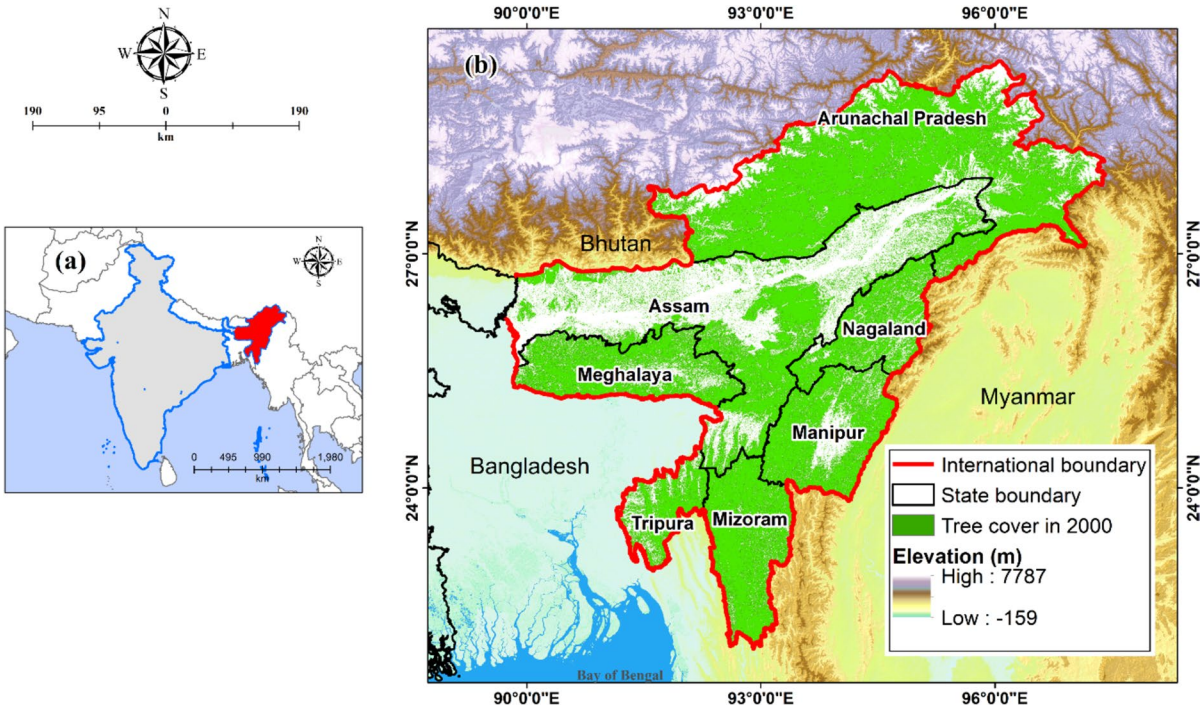

Fig. 1 Geographical location map of the study area in India

Materials and methods

Description of the study area

The study area, encompassing the Seven Sister States of Northeast India (Arunachal Pradesh, Assam, Manipur, Meghalaya, Mizoram, Nagaland, and Tripura), spans longitudinally from 89°41′57″ E to 97°26′16″ E and latitudinally from 21°56′15″ N to 29°29′46″ N, covering approximately 2,55,088 km^2 or 7.8% of India's total area (Fig. 1). This region is strategically positioned, bordered by the Tibetan Autonomous Region of China to the north (1,395 km), Myanmar to the east (1,640 km), Bangladesh to the southwest (1,596 km), and the West Bengal state of India to the west (127.0 km), with Bhutan to the northwest (455 km). The predominant river in this area is the Brahmaputra, which varies in elevation from 2 to 6,698 m above sea level. This region is divided into four geographically distinct zones: the Eastern Himalayas, the Patkai Range, the Brahmaputra Valley, and the Barak Valley (Paul et al., 2020).

According to the Forest Survey of India (2021), 64.66% of the Seven Sisters region is forested, making it one of the twelve biodiversity hotspots in the world. The region's climate is predominantly humid sub-tropical, with hot, humid summers and mild winters. Notably, the region encompasses diverse climatic zones, including areas experiencing severe monsoons, such as Cherrapunji in Meghalaya—the wettest place in the world (Murata et al., 2007), and regions with snow-capped mountains in Arunachal Pradesh (Rehman & Azhoni, 2023). Annual rainfall in the region ranges between 700 mm and 3,500 mm, while the mean daily temperature varies from 2 °C to 25 °C (Vese et al., 2023).

In 2011, the seven states had a total population of approximately 44,876,207, which represents 3.71% of India's total population (Census of India, 2011). The region is home to various tribal groups, including Boro, Karbi, and Rajbanshi in Assam; the Wanchu and Galong in Arunachal Pradesh; the Garo, Khasis, and Karbis in Meghalaya; the Hmar, Paite, Mara, and Pang in Mizoram; the Ao, Sumi, Chang, and Konyak in Nagaland; and the Chakma, Usai, and Reang in Tripura (Ali & Das, 2003; Bajaj, 2011). The forested area in this region has been significantly impacted by the expansion of agriculture. Mandal (2011) revealed that between 1987 and 1997, approximately 1,312 km^2 of forest land was destroyed in Northeast India

due to Jhum or shifting cultivation, a prevalent form of agriculture that involves burning forest land.

Methodology and database

This study employs a combination of geospatial techniques and MCDM models to investigate changes in forest cover and assess areas at risk of deforestation. A comparative analysis of deforestation susceptibility zones is carried out to identify variations in vulnerability across the region. The methodological framework guiding this analysis is depicted in Fig. 2.

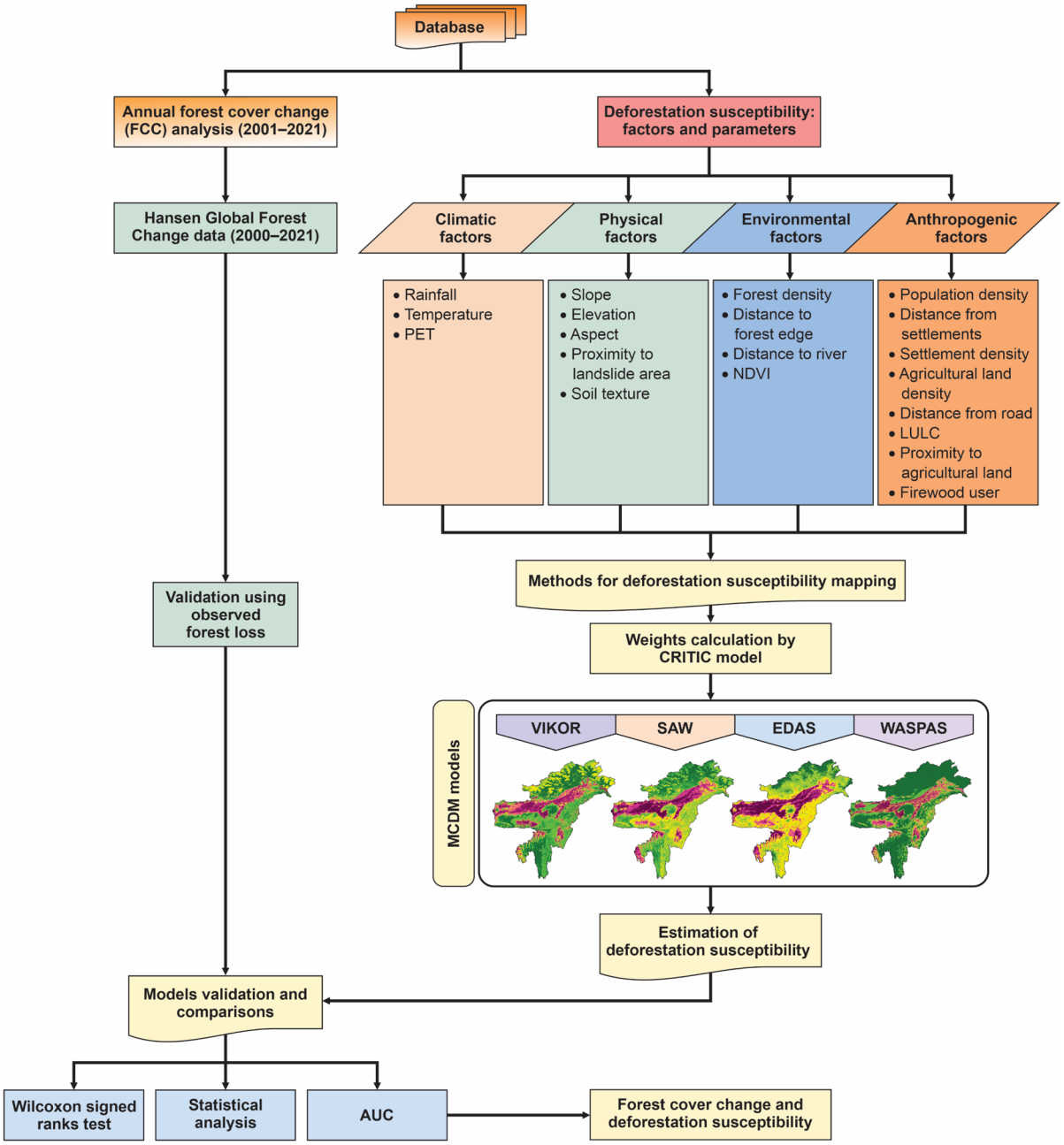

Fig. 2 Methodological framework of the study

Annual forest cover change

Forest cover change dynamics were obtained from the Hansen Global Forest Change (HGFC) data v1.9 product (Hansen et al., 2013), using the Google Earth Engine (GEE) platform. Initially, the data were extracted through the Google Earth Engine platform, which provides extensive access to geospatial datasets, including the HGFC data. This dataset offers global coverage of forest change dynamics, which is crucial for the scope of this research. The processing of this data involved several key steps: (1) Data Extraction: Specific parameters such as forest cover loss, gain, and overall cover were selected and extracted for the study period and region. (2) Data Cleaning and Validation: The data were cleaned to remove any inconsistencies or errors. Validation was performed by cross-referencing with high-resolution satellite imagery and existing forest inventory data to ensure accuracy. (3) Spatial Analysis: This step involved using GIS to overlay forest change data with other environmental and anthropogenic datasets to analyze spatial patterns of forest dynamics.

The reliability of deforestation data provided by the HGFC is widely recognized for its accuracy and comprehensiveness. HGFC utilizes Landsat satellite imagery to monitor global forest cover changes, offering detailed analyses of deforestation. This product combines multitemporal imagery with advanced data processing techniques, contributing to its robustness. Validation studies, comparisons with field data, and the application of change detection models corroborate the quality and reliability of the generated information (Galiatsatos et al., 2020; Wagner et al., 2022). By implementing these rigorous methodologies, the study aims to provide a reliable and accurate assessment of forest changes, minimizing the impact of external factors and errors inherent in the use of satellite-derived datasets like HGFC. These strategies enhance confidence in the findings and ensure that policy recommendations based on this analysis are built on solid and verifiable data.

In the HGFC, canopy closure is defined as tree cover above 5 m. The primary dataset is divided into $10° \times 10°$ tiles, each containing seven files, with a resolution of about 30 m per pixel (Mishra et al., 2022). Two bands from this database were used in the present study: (a) tree cover 2000 (band name: treecover2000) — indicating the proportion of forest cover in the year 2000, ranging from 0 to 100 percent; (b) tree cover loss year (band name: lossyear) — representing annual forest cover loss or a change from forest lands to non-forest lands per year. In the latter band, '0' denotes 'no forest loss,' while values 1 to 21 represent the loss of forest corresponding to each year.

The HGFC data was first imported into the GEE platform, aligning with the boundaries of the study area. The forest cover (FC) area of each cell was then calculated relative to the grid-cell percentage (ranging from 0 to 100) of the treecover2000 band. Twenty-one different forest loss raster images for each year from 2001 to 2021 were extracted from the 'lossyear' band to analyze annual FC loss. In the FC loss raster dataset, values of 0 and 1 signify no loss and loss in that year, respectively. A script to extract these datasets through the GEE was adapted based on the methodology proposed by Santos et al. (2020). After all the raster images were collected, the annual forest loss area and the percentage of the study area were calculated using ArcGIS 10.4.

Deforestation susceptibility: Factors and parameters

The analysis of deforestation susceptibility involves various sensitive parameters, each leaving distinct footprints in geospatial mapping. Selecting appropriate independent variables or explanatory factors represents a critical challenge, as existing literature offers no definitive guidelines for parameter identification (Saha et al., 2021). Techniques such as Multiple regression models, Relief-F tests, Information gain ratio, and probabilistic models aid in this selection, addressing parameter significance and reducing uncertainty. In this study, the multicollinearity diagnostic test method was chosen to ensure the robustness of the analysis by eliminating interdependent variables, thus enhancing model validity (Guria et al., 2024a; Mishra et al., 2024a).

Initially, raster thematic layers for four categories of factors and 20 deforestation susceptibility conditioning parameters were prepared within a GIS environment (Table 1). These parameters were then utilized to comprehensively analyze the drivers of deforestation, providing a nuanced understanding of the complex interactions influencing forest loss,

Table 1 Details of all parameters, methods, and data sources for identification of the deforestation susceptibility zones

Factors	Effective factors	Methods used	Data used	Data sources
Climatic	Rainfall	Inverse Distance Weighted (IDW) $\hat{X}p = \sum_{i=1}^{N} WiXi$ $Wi = \left\{ di^{-a} / \sum_{i=1}^{N} di^{-a} \right\}$	Daily gridded rainfall data (0.25° × 0.25°)	India Meteorological Department (http://imdpune.gov.in)
	Temperature	Inverse Distance Weighted (IDW)	Gridded daily temperature data (1.0°)	India Meteorological Department (http://imdpune.gov.in)
	PET	Inverse Distance Weighted (IDW)	CRU TS v. 4.07	Climatic Research Unit (https://crudata.uea.ac.uk)
Physical	Slope	SRTM digital elevation model	SRTM DEM (1 Arc-Second)	U.S Geological Survey (https://www.usgs.gov)
	Elevation			U.S Geological Survey (https://www.usgs.gov)
	Aspect	Aspect $= 57.29 \times \alpha tan2\left(\left[\frac{dz}{dy}\right] - [dz/dx]\right)$ Where, $dz/dx = ((c + 2f + i) - (a + 2d + g))/8$ $dz/dy = ((g + 2h + i) - (a + 2b + c))/8$ Here, a to i indicates the cell		U.S Geological Survey (https://www.usgs.gov)
	Proximity to the landslide area	Inverse Distance Weighted (IDW)	Vector points	Bhukosh (Geological Survey of India) (https://bhukosh.gsi.gov.in)
	Soil texture	Vector to raster conversion	Vector polygon	
Environmental	Forest density	$Fd = \sum_{i=1}^{n} \frac{F_i}{A}$ F_i = Forest area; A = total area	Landsat images (30 m)	U.S Geological Sps://www.usgs.gov)
	Distance from the forest edge	Euclidean distance buffering	Landsat images (30 m)	U.S Geological Survey (https://www.usgs.gov)
	Distance from river	Euclidean distance buffering	SRTM DEM (1 Arc-Second)	U.S Geological Survey (https://www.usgs.gov)
	NDVI	$NDVI = \frac{(NIR-RED)}{(NIR+RED)}$ NIR = the near-infrared band; RED = red band	Landsat images (30 × 30 m)	U.S Geological Survey (https://www.usgs.gov)

Table 1 (continued)

Factors	Effective factors	Methods used	Data used	Data sources
Anthropogenic	Population density	$Pd = \sum_{i=1}^{n} \frac{P_i}{A}$ P_i= Total Population; A = total area	Census population data	Census of India (https://censusindia.gov.in)
	Distance from settlements	Euclidean distance buffering	Extracted from LULC classes	ESRI LULC (https://www.esri.com)
	Settlement density	$Sd = \sum_{i=1}^{n} \frac{S_i}{A}$ S_i= Settlement area; A = total area	Extracted from LULC classes	ESRI LULC (https://www.esri.com)
	Agricultural land density	$Ald = \sum_{i=1}^{n} \frac{Al_i}{A}$ Al_i= Agricultural land; A = total area	Extracted from LULC classes	ESRI LULC (https://www.esri.com)
	Distance from road	Euclidean distance buffering	Open street road vector layer	Open Street Map (https://www.openstreetmap.org)
	LULC	Deep learning AI land classification model	Sentinel-2 (10 m resolution)	ESRI LULC (https://www.esri.com)
	Proximity to agricultural land	Euclidean distance buffering	Extracted from LULC classes	ESRI LULC (https://www.esri.com)
	Firewood users (per 1000 households)	Inverse Distance Weighted (IDW)	Census data	Census of India (https://censusindia.gov.in)

including socioeconomic factors, land use changes, and policy interventions. This multifaceted approach significantly enhances the accuracy and depth of the research findings. Significant considerations were made concerning the disparities in spatial resolution from various satellite imagery sources. All datasets were prepared at a 30-m resolution and projected using the UTM 45N projection system.

Methods for deforestation susceptibility mapping

Weights calculation by CRITIC model Determining weights is a critical task in any decision-making model, and in this study, weights for all explanatory factors were determined using the Criteria Importance Through Inter-Criteria Correlation (CRITIC) method, which relies on objective weights. Proposed by Diakoulaki et al. (1995), this method does not necessitate weights derived from expert opinions or decision-makers' preferences but instead assigns weights based on contrast strength and conflict intensity among factors (Islam et al., 2022; Qi et al., 2022).

Step 1: A decision matrix X, dimensioned $n \times m$, is first generated:

$$X = \left[X_{ij}\right] = \begin{bmatrix} X_{11} & X_{12} & \cdots & X_{1m} \\ X_{21} & X_{22} & \cdots & X_{2m} \\ \vdots & \vdots & \vdots & \vdots \\ X_{n1} & X_{n2} & \cdots & X_{nm} \end{bmatrix} \quad (1)$$

where n represents alternatives and m refers to criteria; X_{ij} denotes the value of the i^{th} alternative of the j^{th} criterion. A total of 253,316 alternatives across 20 criteria were analyzed.

Step 2: Normalization of matrix X converts factor values to a standard scale between 0 and 1. Before normalization, it is essential to identify beneficial (BC) and non-beneficial (CC) criteria:

$$x_{ij}^{T} = \begin{cases} \frac{x_{ij}-x_j^-}{x_j^+-x_j^-}, x_j^+ \text{ if } j \in BC, \\ \frac{x_j^- - x_{ij}}{x_j^- - x_j^+}, x_j^+ \text{ if } j \in CC, \end{cases} \quad (2)$$

where x_j^+ and x_j^- represent the maximum and minimum values, respectively, for the j^{th} criterion.

Step 3: The standard deviation of each criterion is calculated using Eq. (3). This measure indicates the variability of the criteria:

$$\sigma_q = \sqrt{\frac{\sum_{p=1}^{m}\left(X_{pq}{}^{*} - \overline{X_{pq}{}^{*}}\right)^2}{m}} \quad (3)$$

where $\overline{X_{pq}{}^{*}}$ is the mean value of j^{th} criterion, and m indicates the total number of alternatives. This step is crucial to understand the dispersion within each criterion.

Step 4: A symmetric matrix of dimensions $m \times m$ is constructed, where each element, r_{jk}, represents the linear correlation coefficient between the criterion vectors x_i and x_k. The matrix element r_{jk} indicates the degree of linear relationship between the criteria; a lower value of r_{jk} suggests greater discordance between the criteria j and k, influencing their respective weights.

Step 5: The measure of conflict created by each criterion with respect to the decision context defined by other criteria is computed using Eq. (4):

$$\sum_{k=1}^{m}\left(1 - r_{jk}\right) \quad (4)$$

where m is the total number of alternatives, and r_{jk} is the linear correlation coefficient. This equation quantifies the degree of independence of each criterion, which is pivotal for weighting.

Step 6: Information measures for each criterion are calculated using Eq. (5), which integrates the standard deviation and conflict measures:

$$C_j = \sigma_j \cdot \sum_{k=1}^{m}\left(1 - r_{jk}\right) \quad (5)$$

where C_j denotes the quantity of information conveyed by each criterion, and σ_j is the standard deviation. A higher C_j value indicates a greater contribution of the criterion to the decision-making process due to its uniqueness and information richness.

Step 7: Finally, the objective weights of each criterion are determined using Eq. (6):

$$w_j = \frac{C_j}{\sum_{k=1}^{m} C_k} \quad (6)$$

where w_j represents the objective weight assigned to each criterion. This weighting method prioritizes criteria with higher variability and lower correlations with others, aligning with the principles of the CRITIC method (Diakoulaki et al., 1995; Slebi-Acevedo et al., 2020).

For precise spatial analysis in CRITIC models, the 'Fishnet tool' was preferred over the 'Create random points tool' for generating spatially distributed data points. Values for each criterion were extracted for about 253,316 points using the 'Extract Multi Values to Points' tool of ArcGIS v10.4. The resulting metrics were processed through 'Excel v2016' to determine the final weights.

SAW model Simple Additive Weighting (SAW) (Hwang & Masud, 2012) is a well-known MCDM method. This model is computed by aggregating the values and weights of each criterion. In this scenario, relative weight does not need to be calculated; instead, the weight is directly assigned by decision-makers using either a subjective or objective method (Ameri et al., 2018; Bhattacharya et al., 2020). The following steps were implemented to calculate the SAW model in the current study (Tzeng & Huang, 2011).

Step 1: Initially, the decision-matrix table (X) is created using Eq. (1).

Step 2: The subsequent step is to normalize the decision-matrix table (X). For this purpose, Eq. (2) is used.

Step 3: The weighted normalized decision matrix (V_{ij}) is determined using Eq. (7):

$$V_{ij} = R_{ij} \times w_j \quad (7)$$

where V_{ij} indicates the weighted normalized decision matrix and w_j refers to the weight of the j^{th} criterion.

Step 4: The final step involves calculating the significance degree of each alternative. In this case, Eq. (8) is utilized:

$$S_j = \sum_{i=1}^{m} w_j v_{ij} \tag{8}$$

where S_j signifies the significance degree of the i^{th} alternative.

WASPAS model The Weighted Aggregates Sum Product Assessment (WASPAS) was proposed by Zavadskas et al. (2012). This model is one of the newest robust MCDM approaches, which combines the weighted product model (WPM) and the weighted sum model (WSM) to enhance the accuracy of model output results. According to Wang et al. (2021), the WASPAS model provides better results compared to the two separate models, and presently, this model is being utilized in various fields (Slebi-Acevedo et al., 2020). The detailed procedure for the model's calculation is explained as follows:

Step 1: Firstly, the decision-matrix table (X) is created by applying Eq. (1).
Step 2: In this step, the beneficial and non-beneficial criteria are identified, and the decision matrix is normalized using Eq. (2).
Step 3: According to the WSM, the total relative importance of the i^{th} alternative is determined by Eq. (9).

$$Q_i^{(1)} = \sum_{j=1}^{n} \bar{x}_{ij} w_j \tag{9}$$

where $Q_i^{(1)}$ is the WSM, and w_j is the weight of the j^{th} criteria. In this case as well, the weight of each category is obtained from the CRITIC method.
Step 4: Similarly, the total relative importance of the i^{th} alternative with respect to the WPM is determined by Eq. (10).

$$Q_i^{(2)} = \prod_{j=1}^{n} \left(\bar{x}_{ij}\right)^{w_j} \tag{10}$$

where $Q_i^{(2)}$ is the WPM, and w_j is the weight of the j^{th} criteria.

Step 5: To increase the accuracy and effectiveness of the decision-making approach, two separate models, WSM and WPM, have been combined. The integrated WASPAS model is determined by applying Eq. (11).

$$Q_i = \lambda Q_i^{(1)} + (1-\lambda) Q_i^{(2)} = \lambda \sum_{j=1}^{n} \bar{x}_{ij} w_j + (1-\lambda) \prod_{j=1}^{n} \left(\bar{x}_{ij}\right)^{w_j} \quad (\lambda = 0, 0.1, \ldots, 1). \tag{11}$$

In this study, experimentation with varying lambda (λ) values was conducted, testing the range from 0.1 to 0.9 in increments of 0.1. This was done to analyze the stability and sensitivity of the alternative rankings produced by the WASPAS model. A value of 0.5 was chosen to minimize unintended errors, as recommended by Zavadskas et al. (2012). Based on these results, a λ value that balances the features of both the sum and product models was selected for the final analysis to ensure a fair evaluation of all alternatives. This balanced approach was deemed most appropriate for addressing the complexity and multidimensional nature of the decision-making scenario in this study.

VIKOR model The *VlseKriterijumska optimizacija I Kompromisno Resenje* (VIKOR) model is a significant method that concentrates on selecting and ranking a set of options with contradictory criteria (Opricovic, 1998). This model constructs a multicriteria ranking index by quantifying the closest solution to the ideal (Bera et al., 2020). This is done through several steps:

Step 1: Initially, the decision-matrix table (X) is created by applying Eq. (1).
Step 2: Calculation of the ideal best value (f_i^*) and ideal worst value (f_i^-) for both beneficial and non-beneficial criteria. If the j^{th} criterion is beneficial, then the ideal best value should be the maximum, and the ideal worst should be the minimum, and vice versa.

$$f_i^+ = \left\{ \begin{matrix} \max\limits_i f_{ij} & \text{for benefit criterion} \\ \min\limits_i f_{ij} & \text{for cost criterion} \end{matrix} \right\}, j = 1, \ldots m; i = 1, \ldots n, \tag{12}$$

$$f_i^- = \left\{ \begin{array}{ll} \min\limits_i f_{ij} & \text{for benefit criterion} \\ \max\limits_{ij} & \text{for cost criterion} \end{array} \right\}, j = 1, \ldots m; i = 1, \ldots n. \quad (13)$$

Step 3: Calculate the utility measure index (S_j) using Eq. (14).

$$S_j = \sum_{i=1}^{n} w_i \left(f_i^* - f_{ij}\right) / \left(f_i^* - f_i^-\right) \quad (14)$$

where n is the number of criteria, w_i is the weight of the j^{th} criterion, f_i^* is the ideal best value, f_i^- is the ideal worst value, and f_{ij} is the value of the j^{th} criterion of the i^{th} alternatives.

In the application of the VIKOR model within this study, specific methodologies were employed to ascertain the optimal benefit values (f_i^*) and the least favorable cost values (f_i^-). These values are critical for evaluating the compromise solution that provides maximum group utility for the majority and minimum individual regret for the opponent. The normalization technique was used to determine f_i^* and f_i^-. While this involves normalization in the sense of scaling values to a common range relative to the best and worst possible values, its primary purpose is to compute a utility measure for each alternative, rather than to standardize data. This technique helps mitigate the impact of differing measurement scales and distributions across the various criteria, ensuring that the VIKOR methodology provides a fair and balanced assessment of all alternatives based on their performance. The choice of normalization technique can significantly influence the results of the VIKOR analysis. Therefore, the selection is based on the specific characteristics of the data, including the scale of measurement, the presence of outliers, and the desired sensitivity to changes in input values. Each technique has its advantages in handling specific types of data, and in this study, considerations were made to choose the most appropriate method that aligns with the overall goal of achieving a robust and equitable multicriteria decision-making process.

Step 4: Calculate the regret measure index (R_j) by applying Eq. (15).

$$R_j = \max_i \left[w_i \left(f_i^* - f_{ij}\right) / \left(f_i^* - f_i^-\right) \right] \quad (15)$$

Step 5: Determine the value of S^* and R^* using Eq. (16).

$$\begin{aligned} S^* &= \min_j S_j, S^- = \max_j S_j \ [j = 1, 2, \ldots .m] \\ R^* &= \min_j R_j, R^- = \max_j R_j \ [j = 1, 2, \ldots .m] \end{aligned} \quad (16)$$

where S^* and R^* refer to the minimum values of S_j and R_j, respectively; S^- and R^- refer to the maximum values of S_j and R_j, respectively.

Step 6: Compute the Q_j value for the Performance Score by applying Eq. (17).

$$\begin{aligned} Q_j &= v\left(S_j - S^*\right) / (S^- - S^*) \\ &+ (1 - v)\left(R_j - R^*\right) / (R^- - R^*) \end{aligned} \quad (17)$$

where v represents the weight of maximum group utility strategies; $(1 - v)$ is the weight of the individual regret.

When applying the VIKOR model, the calculation of the regret index (or regret measure index) can face challenges due to large fluctuations between criteria, especially when the criteria have varying units or scales of measurement. Such fluctuations can disproportionately influence the regret measure, potentially leading to skewed or biased decision outcomes. In this study, there were no issues with fluctuations because we addressed this by performing the normalization process S_j using Eq. (14).

EDAS model The Evaluation Based on Distance from Average Solution (EDAS) (Ghorabaee et al., 2015a) is a well-regarded MCDM method widely used to evaluate based on Positive Distance from an Average (PDA) and Negative Distance from an Average (NDA) as per beneficial and non-beneficial criteria. The steps of the EDAS method are as follows.

Step 1: The first step focuses on creating the decision-making matrix (X) by applying Eq. (1).

Step 2: Compute the average solution (AV_j).

$$AV_j = \frac{\sum_{i=1}^{n} X_{ij}}{n} \quad (18)$$

Step 3: Determine the PDA_{ij}.

Equation (19) is applied for beneficial criteria.

$$PDA_{ij} = \frac{max\left(0, \left(X_{ij} - AV_j\right)\right)}{AV_j}, \quad (19)$$

Equation (20) is applied for non-beneficial criteria

$$PDA_{ij} = \frac{max\left(0, \left(AV_j - X_{ij}\right)\right)}{AV_j} \quad (20)$$

Step 4: Determine the negative distance from the average (NDA_{ij}).
Equation (21) is applied for beneficial criteria.

$$NDA_{ij} = \frac{max\left(0, \left(AV_j - X_{ij}\right)\right)}{AV_j} \quad (21)$$

Equation (22) is applied for non-beneficial criteria.

$$NDA_{ij} = \frac{max\left(0, \left(X_{ij} - AV_j\right)\right)}{AV_j} \quad (22)$$

Step 5: Calculate the weighted sum of PDA_{ij} among all alternatives.

$$SP_i = \sum_{j=1}^{m} w_j PDA_{ij} \quad (23)$$

where Sp_i refers to the weighted sum of PDA_{ij}, and w_j represents the weight of the j^{th} criterion.
Step 6: Calculate the weighted sum of NDA_{ij} among all alternatives.

$$SN_i = \sum_{j=1}^{m} w_j NDA_{ij} \quad (24)$$

where Sn_i refers to the weighted sum of NDA_{ij}.
Step 7: Determine the normalization of the values of SP_i and SN_i for all alternatives.

$$\begin{aligned} NSP_i &= \frac{SP_i}{\max\limits_i\left(SP_i\right)} \\ NSN_i &= 1 - \frac{SN_i}{\max\limits_i\left(SN_i\right)} \end{aligned} \quad (25)$$

where NSP_i and NSN_i represent the normalized values of SP_i and SN_i, respectively.
Step 8: Determine the appraisal score (AS_i) for all alternatives.

$$AS_i = \frac{1}{2}\left(NSP_i + NSN_i\right) \quad (26)$$

Step 9: Finally, the alternatives need to be ranked according to the decreasing order of the appraisal score (AS_i). The best choice among the alternatives will have the maximum value of AS_i (Ghorabaee et al., 2015b).

The concern regarding potential deviations caused by the computation of PDA and NDA when utilizing the EDAS model is important to address. The EDAS methodology inherently mitigates these issues through its structured steps. By normalizing the distances and computing the weighted sums of PDA and NDA (Eq. 25), the model reduces the risk of any single criterion disproportionately influencing the overall evaluation. Moreover, the calculation of the final appraisal score (AS_i), which combines these normalized values, ensures that the rankings of alternatives are robust and unbiased. Therefore, although deviations might occur due to varying units or scales of criteria, the EDAS model's design effectively balances these differences to provide reliable and consistent evaluation outcomes.

Estimation of deforestation susceptibility

Deforestation susceptibility estimation was performed using 253,316 samples (X,Y) where deforestation instances were recorded in the HGFC product data. Subsequently, the samples were used as input data in the four MCDM models (Q_j – VIKOR, AS_i – EDAS, Q1 – SAW, and Q2 – WASPAS). Then, the sample points were used to generate a raster map of deforestation susceptibility zones for each MCDM using the Inverse Distance Weighting (IDW) interpolation technique.

The final deforestation susceptibility maps using the VIKOR, SAW, EDAS, and WASPAS models were categorized into five distinct classes: "very low," "low," "medium," "high," and "very high." In this study, the categorization of deforestation was developed using equal intervals, which allowed for the reduction of differences within each class and the maximization of differences between classes (Saha et al., 2022).

The choice to employ the IDW method for interpolating points in creating a deforestation

vulnerability map was based on several considerations that align with the specific needs and constraints of this study. The decision was informed by comparing IDW with other common interpolation methods such as Spline, Kriging, and Natural Neighbor, evaluating criteria including simplicity, data requirements, computational efficiency, and suitability to the data characteristics. The justification for using IDW are (a) simplicity and interpretability, (b) data suitability, (c) computational efficiency, and (d) control over influence.

The comparison with methods such as Spline reveals that their results are unrealistic in areas where deforestation is highly non-uniform and are sensitive to outliers, which can distort the vulnerability map where deforestation patterns are irregular. Kriging, while useful, requires a well-defined model of spatial correlation and extensive data preprocessing to determine the semivariogram, which was not optimal given the variability and uncertainty in deforestation data. The Natural Neighbor method can be less effective than IDW when the data points are unevenly distributed across the study area, a common issue in deforestation data. Thus, the IDW method was selected as it provides a balance between accuracy, ease of use, and computational demands, making it highly suitable for creating a deforestation vulnerability map with the available data. This method allows for effective representation of local variations in deforestation risk without the need for complex model specifications or assumptions inherent in other interpolation techniques. In this study, multivariate analysis was not performed because it was not the objective to analyze correlations among independent variables.

Models validation and comparisons

Validating prediction results is a crucial task, as researchers and policymakers derive significant interpretations from these results. The calibration process involved applying the Receiver Operating Characteristic (ROC), Area Under the Receiver Operating Characteristic (AUC) curve, statistical analysis, and Wilcoxon signed-rank tests.

Receiver operating characteristic (ROC) and area under the receiver operating characteristic (AUC) curve

The ROC curve is a graphical representation that plots sensitivity (or True Positive Rate, TPR) against 1 – Specificity (or False Positive Rate, FPR) at various threshold settings. The x-axis represents 1 – Specificity, indicating the models' error predictions, while the y-axis displays sensitivity, reflecting the models' accuracy and effectiveness (Arabameri et al., 2020; Bhutia et al., 2024).

To ascertain the significance of individual factors within MCDM models, sensitivity analysis was conducted. This method allowed for the identification of how variations in input parameters affect model outputs, thereby highlighting the factors with the most significant impact on the results. Techniques such as Sensitivity, Specificity, Accuracy, AUC, and Precision were employed. Each criterion was removed one at a time to observe the effect on the overall decision score, providing insights into the relative importance and sensitivity of each criterion.

The AUC analysis was utilized to assess the ability of the MCDM models to effectively distinguish between deforested and non-deforested areas. The AUC values provide a quantitative measure of model performance in terms of sensitivity and 1 – specificity, classified as follows: 0.5–0.6 indicates poor discrimination; 0.6–0.7, fair; 0.7–0.8, acceptable; 0.8–0.9, good; and 0.9–1, excellent (Rasyid et al., 2016).

Sensitivity analyses were rigorously performed to evaluate the impact of each factor on the model results within the context of this study. Sensitivity analysis is crucial for understanding how changes in input parameters affect model outcomes, thereby providing insights into the stability and robustness of the decision-making process. This evaluation was based on the analysis of 500 points identified as deforested and 500 points as non-deforested to verify the accuracy of the predictions by MCDM models. The evaluation metrics, including sensitivity, specificity, accuracy, and precision, are quantified through Eqs. (27) to (31).

$$Specificity = 1 - \frac{TN}{(TN + FP)} \tag{27}$$

$$\text{Sensitivity} = \frac{TP}{(TP + FN)} \tag{28}$$

$$AUROC = \sum_{k=1}^{n} \left(F_{k+1} - F_k\right)\left(\frac{T_{k+1} + T_k}{2}\right) \tag{29}$$

$$Accuracy = \frac{TP + TN}{TP + TN + FP + FN} \tag{30}$$

$$Precision = \frac{TP}{TP + FP} \tag{31}$$

where *TP* refers to true positives, representing pixels correctly classified as deforestation. *TN* denotes true negatives, indicating pixels correctly classified as non-deforestation. *FP* stands for false positives, which are pixels incorrectly classified as deforestation, and *FN* is false negatives, referring to pixels incorrectly classified as non-deforestation. F_k represents the false positive rate (1 – Specificity) at each threshold, and T_k denotes the sensitivity (True Positive rate) at each threshold (Guria et al., 2024b).

Regarding the consideration of climate factors, temperature, and precipitation were integrated into the MCDM models through their direct and indirect impacts on forest area change. These climate variables were modeled as criteria within the MCDM framework, with their weights determined based on historical significance and projected changes. The impact of these factors was assessed using regression analysis to correlate changes in climate variables with alterations in forest cover. This assessment was supported by spatial data analysis, which visualized the distribution and magnitude of these changes across the study area. These methodological enhancements and the comprehensive evaluation of climate factors provide a robust framework for understanding and predicting the dynamics of forest area change under varying climatic conditions. This approach contributes valuable insights into the fields of environmental management and policy formulation.

Statistical analysis

In evaluating the robustness of the deforestation susceptibility models, it is crucial to understand that a lower False Negative Rate (FNR, or miss rate) is indicative of higher model accuracy. Conversely, for the remaining metrics utilized in this study—including Cohen's Kappa index, True Negative Rate (TNR), Positive Predictive Value (PPV), False Discovery Rate (FDR), Negative Predictive Value (NPV), False Omission Rate (FOR), F-score, Matthew's Correlation Coefficient (MCC), Yule's Q, and True Skill Statistics (TSS)—higher values correspond to enhanced model accuracy (Arabameri et al., 2020).

Wilcoxon signed-rank tests

Non-parametric statistical hypothesis tests, specifically the Wilcoxon signed-rank tests (Wilcoxon, 1949), were applied to assess the significance of differences among the performances of the four types of MCDM models utilized in this study. These tests help in determining the acceptability of each model based on their ability to predict deforestation susceptibility accurately. The null hypothesis for this analysis posits that there is no significant difference in the performance (in terms of prediction accuracy) among the four MCDM models. Statistical significance is evaluated using the *p*-value and Z-value; if the *p*-value is less than 0.05 and the Z-value exceeds ± 1.96, the null hypothesis is rejected. Such an outcome would indicate a significant difference in the performance levels of the MCDM models regarding their effectiveness in creating deforestation susceptibility maps.

Results

Forest cover change analysis (2001–2021)

Table 2 presents the total forest cover in 2000, the total annual forest loss since 2000, the percentage, and mean forest loss for seven states of Northeast India. Our analysis found that the highest amount of forest cover in 2000 was observed in Arunachal Pradesh (64,773.57 km^2), while the lowest was in Tripura (7,677.95 km^2). The highest percentage of forest cover in terms of geographical area is observed in Mizoram (94%), followed by Nagaland (83%). Even though Assam ranks second in terms of total forest cover (32,535.32 km^2), in contrast, the state has the lowest forest cover (41%) relative to its geographical area.

Table 2 Forest cover loss between 2001 and 2021 in Northeast India

States		Assam	Nagaland	Mizoram	Arunachal Pradesh	Manipur	Meghalaya	Tripura	Total
Tree cover 2000 (km^2)		32,535.32	13,678.29	19,751.04	64,773.57	17,815.25	18,145.70	7677.95	174,377.12
Total area (km^2)		78,438	16,579	21,081	83,743	22,327	22,429	10,491	2,55,088
Forest cover by area (%)		41	83	94	77	80	81	73	68
Loss per year (km^2)	2001	70.23	127.34	50.78	89.18	45.29	46.62	30.82	460.25
	2002	84.15	81.15	45.80	71.77	43.35	36.98	19.09	382.29
	2003	60.64	79.91	41.61	70.84	53.86	24.24	13.18	344.28
	2004	134.31	102.47	51.73	132.73	54.19	58.55	29.44	563.42
	2005	86.10	91.85	50.05	91.23	49.90	43.68	15.08	427.90
	2006	95.26	71.78	38.52	100.96	54.74	53.54	62.10	476.90
	2007	126.14	50.99	16.93	99.67	43.80	67.38	58.63	463.55
	2008	165.20	67.66	38.72	113.03	59.82	74.04	53.03	571.52
	2009	163.09	75.18	43.73	92.81	63.04	52.64	50.73	541.22
	2010	110.03	49.79	29.71	61.26	44.09	67.49	33.96	396.32
	2011	151.97	74.86	34.62	132.15	65.06	57.90	25.72	542.28
	2012	179.47	146.13	75.20	157.59	93.67	62.49	21.49	736.02
	2013	105.97	172.92	121.78	112.90	145.64	96.36	31.52	787.09
	2014	286.60	260.27	207.92	161.84	193.16	218.48	62.72	1390.99
	2015	254.16	261.51	153.21	153.72	184.67	194.13	48.84	1250.25
	2016	308.86	292.70	390.75	234.77	255.36	245.22	61.87	1789.54
	2017	209.40	335.31	473.76	235.27	235.46	266.57	169.34	1925.10
	2018	178.12	250.54	296.55	144.04	181.47	173.11	84.81	1308.64
	2019	134.60	178.41	274.94	124.61	172.45	151.51	118.78	1155.29
	2020	221.49	242.91	294.80	162.25	196.18	157.90	127.21	1402.74
	2021	224.80	192.68	317.65	178.24	206.35	130.94	125.05	1375.71
Total loss (km^2)		3350.59	3206.35	3048.76	2720.87	2441.55	2279.79	1243.41	18,291.31
Total loss (%)		18.32	17.53	16.67	14.88	13.35	12.46	6.80	100
Loss since 2000 (%)		10.30	23.44	15.44	4.20	13.70	12.56	16.19	10.49
Mean loss (km^2)		159.55	152.68	145.18	129.57	116.26	108.56	59.21	871.01

The analysis indicates that a significant amount (10.49%) of the total forest area has been destroyed in the last two decades. As shown in Fig. 3, the entire state of Northeast India has been affected by forest loss. During this period, the highest amount of forest loss has occurred in Nagaland (23.44%), with more than 15% of forest cover having been lost in the states of Mizoram and Tripura. Arunachal Pradesh (4.20%) has lost the least amount of forest cover relative to its total geographical area. However, according to our analysis, the total forest loss in this state is 2720.87 km^2. The highest mean change rate of 159.55km^2/year was recorded in Assam, while the lowest mean change rate of 59.21km^2/year was found in Tripura.

This study investigated the recent (2001–2021) trends in forest loss in seven states. Figure 3(i) reveals a trend of annual forest loss for all seven states. Here, a positive upward trend ($R^2 = 0.6984$) is visible. Furthermore, analysis indicates a marked escalation in deforestation rates beginning in 2014, highlighting an increasing trend in forest cover loss. The most consistent loss of forest land has been observed in Manipur ($R^2 = 0.7591$) as seen in Fig. 3(f). In the other states, the rate of forest loss has been observed to increase over the years with a decrease in some years. For example, Assam lost the most forest area (308.86 km^2) in 2016, but this figure dropped to 134.60 km^2 in 2019 as shown in Fig. 3(b). Despite this, Table 2 and Fig. 3(g) show

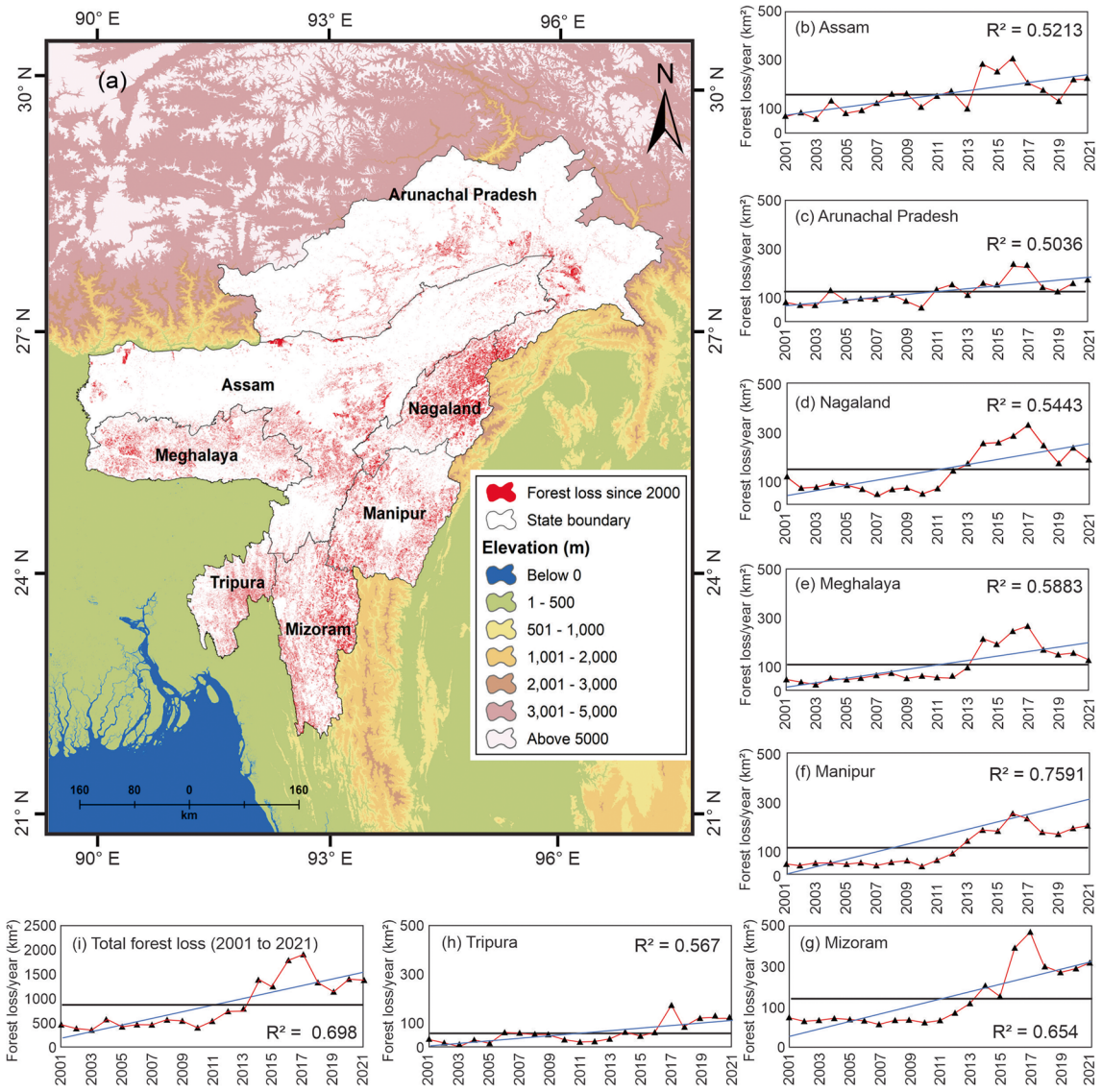

Fig. 3 Forest cover dynamics: (**a**) total forest loss since 2000, and state-wise trends in forest cover during the last two decades for (**b**) Assam, (**c**) Arunachal Pradesh, (**d**) Nagaland, (**e**) Meghalaya, (**f**) Manipur, (**g**) Mizoram, (**h**) Tripura, and (**i**) total forest losses from 2001 to 2021

that Mizoram (473.76 km^2) recorded the highest loss of forest cover in a single year (2017) among all states. The gradual trend of deforestation is least observed in Arunachal Pradesh ($R^2 = 0.5036$), as shown in Fig. 3(c). Deforestation has also been observed in Tripura ($R^2 = 0.567$), but it is limited, as depicted in Fig. 3(h). The spatiotemporal change of forest cover in the Northeastern states of India is shown in Fig. 4.

Deforestation susceptibility assessment

Multicollinearity analysis of selected independent variables

In the context of the multivariate analysis conducted within this study, a thorough examination of potential correlations among independent variables was undertaken. Multicollinearity diagnostics were applied to

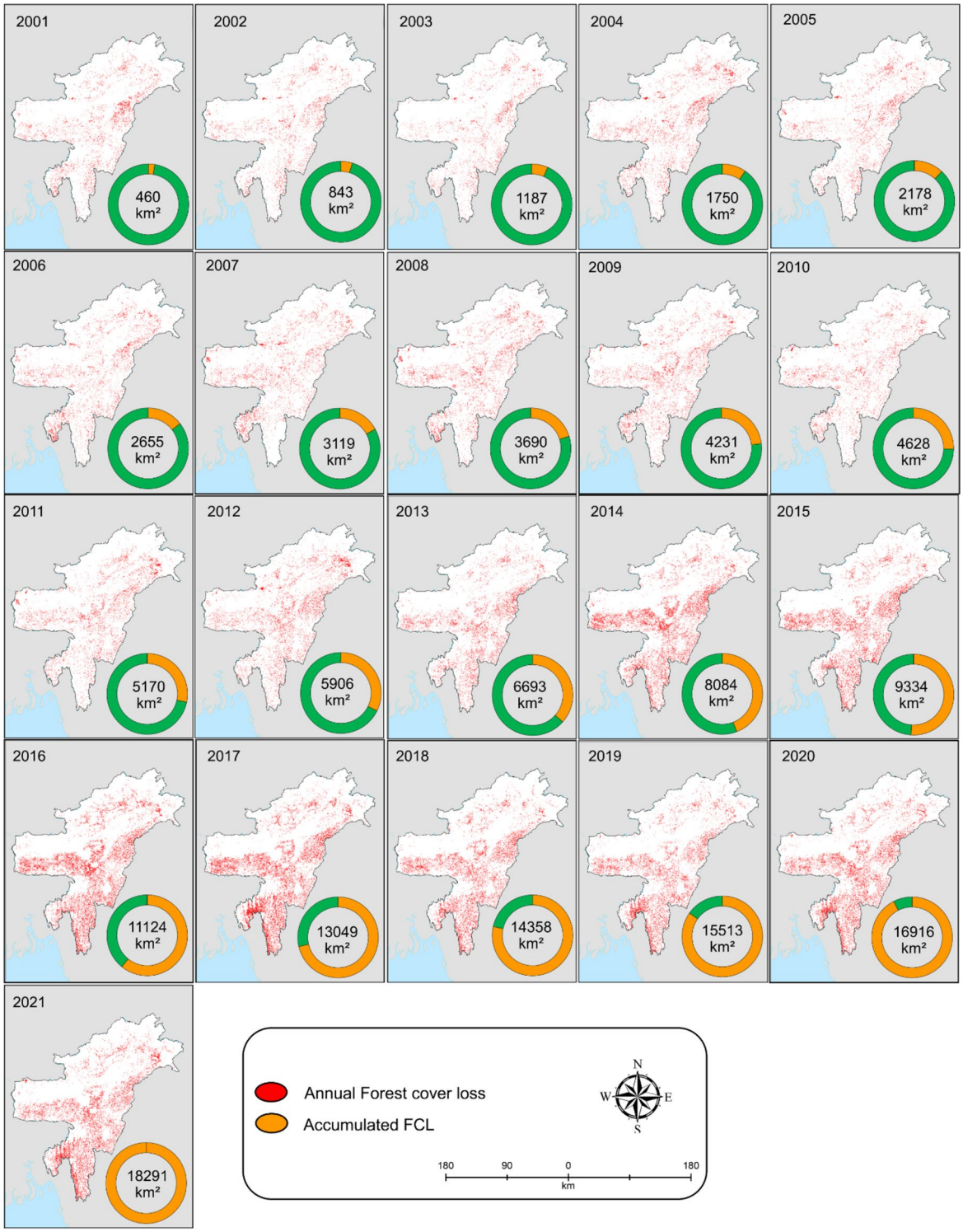

Fig. 4 Spatiotemporal changes in forest cover loss from 2001 to 2021 are depicted. The annual distribution of forest loss is highlighted in red. Circles overlaid on the map represent the cumulative forest cover loss for each year, illustrating the progression and concentration of deforestation over the two-decade period

Table 3 Multicollinearity analysis results

Parameters	Collinearity statistics		Parameters	Collinearity statistics	
	Tolerance	VIF		Tolerance	VIF
Elevation	0.11	8.83	Rainfall	0.42	2.36
Temperature	0.12	8.13	Dist. from road	0.43	2.35
PET	0.13	7.87	Firewood user	0.45	2.22
Agricultural density	0.25	3.94	Slope	0.49	2.06
Forest density	0.26	3.85	Landslide place	0.53	1.88
LULC	0.28	3.53	Settlement density	0.61	1.64
NDVI	0.30	3.37	Soil	0.74	1.36
Population density	0.31	3.19	Dist. from forest edge	0.77	1.3
Prox. to agri. lands	0.32	3.17	Dist. from river	0.94	1.06
Dist. from settlements	0.33	3.07	Aspect	0.96	1.04

assess potential collinearity among 20 parameters, ensuring the reliability of statistical estimates for each independent variable. The multicollinearity test results, presented in Table 3, indicated that with all variance inflation factor (VIF) values being less than 10 and all tolerance values greater than 0.1, there are no significant collinearity issues among the selected explanatory parameters. This outcome supports the reliability of the variables' statistical estimates in the deforestation susceptibility model, although it does not directly measure the model's overall uncertainty.

Evaluation matrix

In the current study, the generation of the final deforestation susceptibility maps using the VIKOR, SAW, EDAS, and WASPAS methods was based on 20 explanatory factors. Given that these MCDM techniques do not operate on a per-pixel basis, we used the 'Create Fishnet' tool in ArcGIS v10.4 to generate 253,316 sample points to prepare the evaluation matrix for these four models. Subsequently, we extracted the values of these points from each thematic layer. The evaluation matrix table comprises 253,316 rows (representing sample points) and 20 columns (representing factors). Assigning weights to the deforestation explanatory criteria is a crucial task in this process. Therefore, we utilized the objective-based CRITIC statistical method to calculate the weights for each parameter. Of the total 20 explanatory factors, 10 were classified as beneficial criteria (BC), while the remaining 10 factors were categorized as non-beneficial (NB) or cost criteria (CC), as shown in Table 4. In this study, the highest weights were calculated for aspect and forest density (10%), followed by soil (9%), slope (7%), LULC, agricultural density, NDVI (6%), proximity to landslide area, rainfall, and PET (5%), temperature, elevation and proximity to agricultural land (4%), settlement density, population density, distance to road, and distance to river (3%), and distance to settlements, distance to forest edge, and fire-wood user (2%). All the statistics derived from the SAW, WASPAS, VIKOR, and EDAS models are shown in Table 5.

Generation of deforestation susceptibility maps

The final deforestation susceptibility maps using VIKOR, SAW, EDAS, and WASPAS techniques are shown in Fig. 5. and Table 6. It segments the raster data naturally, reducing the differences within each class and maximizing the differences between classes (Saha et al., 2022). It should be noted that for SAW, WASPAS, and EDAS, a higher model output value indicates a very high deforestation susceptibility zone, while a lower value suggests a very low susceptibility zone. In contrast, for the VIKOR model, an inverse relationship is observed, where a lower value represents a high deforestation susceptibility zone, and a higher value represents a low susceptibility zone. A composite graph (Fig. 6) shows the area distribution by deforestation susceptibility category, as derived from different models for the seven states of Northeast India.

Table 4 Evaluation matrix of VIKOR, EDAS, SAW, and WASPAS

Parameters	LULC	Soil	AD	Aspect	Slope	PET	FWU	Temp	PD	SD	NDVI	Elevation	PAL	LP	R	DFE	DR	Dro	DS	FD
Category	**BC**	**BC**	**BC**	**BC**	**BC**	**BC**	**BC**	**BC**	**BC**	**BC**	**CC**	**CC**	**CC**	**CC**	**CC**	**CC**	**CC**	**CC**	**CC**	**CC**
Weight	**0.06**	**0.09**	**0.06**	**0.10**	**0.07**	**0.05**	**0.02**	**0.04**	**0.03**	**0.03**	**0.06**	**0.04**	**0.04**	**0.05**	**0.05**	**0.02**	**0.03**	**0.03**	**0.02**	**0.10**
S1	2	4	0.00	− 1.00	0.00	34.37	833.98	19.83	60.21	0.03	0.80	247.00	635.69	26,523.20	1426.98	9514.73	780.00	1303.88	1583.19	1.00
S2	2	4	0.00	− 1.00	0.00	34.27	1082.98	21.93	140.38	0.00	0.51	1465.00	577.06	3704.12	2868.49	300.00	120.00	2568.46	271.66	0.06
S3	2	1	0.00	− 1.00	0.00	32.83	711.82	19.86	470.22	0.22	0.39	772.00	680.15	2545.58	1485.61	270.00	660.00	1176.52	1259.29	0.20
S4	2	1	0.00	− 1.00	0.00	37.08	1385.88	24.13	584.20	0.04	0.69	54.00	649.00	29,620.80	2005.54	1462.63	1317.95	863.77	1668.17	1.00
S5	2	4	0.00	− 1.00	0.00	35.63	1145.34	22.50	216.54	0.08	0.57	130.00	517.88	71,539.20	1535.21	848.53	466.69	2753.47	1350.00	0.22
….																				
S253312	2	1	0.01	178.46	82.93	30.51	818.44	14.98	55.15	0.02	0.60	2085.00	6264.83	50,984.70	1288.06	0.00	420.00	5538.56	5778.17	0.44
S253313	2	1	0.01	185.89	82.94	29.76	776.09	11.23	73.32	0.01	0.29	3327.00	39,389.60	77,226.40	1092.44	9150.15	424.26	26,593.30	22,987.50	0.16
S253314	1	1	0.04	287.86	83.20	29.76	751.46	10.98	92.69	0.03	0.11	4545.00	47,960.70	57,682.20	1120.01	7004.98	870.00	27,700.90	20,335.00	0.17
S253315	1	1	0.04	165.24	84.65	29.76	746.92	10.93	91.14	0.02	0.15	4707.00	47,941.80	56,940.40	1117.32	7406.84	120.00	26,720.20	21,070.30	0.17
S253316	2	1	0.16	297.12	84.83	30.20	772.47	13.58	38.55	0.01	0.41	2659.00	35,242.70	48,115.50	1121.18	466.69	445.98	14,221.40	10,952.60	0.05

LULC = Land Use and Land Cover, Soil = Soil Texture, AD = Agricultural Density, PET = Potential Evapotranspiration, FWU = Firewood User, Temp = Mean Temperature, PD = Population Density, SD = Settlement Density, NDVI = Normalized Difference Vegetation Index, PAL = Proximity to Agricultural Land, LP = Landslide Places, R = Rainfall, DFE = Distance from Forest Edge, DR = Distance from River, Dro = Distance from Road, DS = Distance from Settlement

Table 5 Statistics of the SAW, WASPAS, VIKOR, and EDAS models

#	SAW (Q1)	WASPAS	VIKOR			EDAS		
			Sj	Rj	Qj	NSPi	NSNi	Asi
S1	0.41	0.20	0.59	0.10	0.84	0.18	0.73	0.46
S2	0.51	0.25	0.49	0.10	0.74	0.34	0.78	0.56
S3	0.46	0.23	0.54	0.10	0.78	0.33	0.81	0.57
S4	0.38	0.19	0.62	0.10	0.87	0.20	0.75	0.47
S5	0.51	0.26	0.49	0.10	0.74	0.28	0.80	0.54
….								
S253312	0.48	0.24	0.52	0.09	0.65	0.40	0.80	0.60
S253313	0.46	0.23	0.54	0.09	0.67	0.45	0.40	0.42
S253314	0.47	0.24	0.53	0.09	0.66	0.52	0.37	0.44
S253315	0.44	0.22	0.56	0.09	0.69	0.47	0.37	0.42
S253316	0.54	0.27	0.46	0.09	0.59	0.55	0.66	0.60

Deforestation susceptibility analysis using the VIKOR model The VIKOR model has been used to demarcate deforestation susceptibility zones in Northeast India. The predicted map model has been categorized into five classes (Fig. 5(a)) based on different threshold values: very low (0.78–1.00), low (0.58–0.78), moderate (0.40–0.58), high (0.22–0.40), and very high (0–0.22). The areas classified as very high and high deforestation susceptibility zones were observed in the middle part, southwestern, and southeastern parts of the study area. The spatial distribution of the deforestation susceptibility zones, from "very high" to "very low," showed coverage areas of 8.76%, 11.80%, 18.59%, 32.57%, and 28.28%, respectively. According to the susceptibility maps, Assam, Tripura, and Arunachal Pradesh were very susceptible to deforestation, with the zones from "medium" to "very high" susceptibility observed to be most extensive in these states. Conversely, Mizoram, Nagaland, and Manipur were less susceptible to deforestation.

Deforestation susceptibility analysis using the SAW model The deforestation probability using the SAW model was determined based on the relative weight assigned by the CRITIC method. The results of the SAW model were classified into five different categories: very low (0.24–0.4), low (0.41–0.45), moderate (0.46–0.52), high (0.53–0.6), and very high (0.61–0.78). Areas of very high (10.96%) and high (13.84%) deforestation susceptibility were identified in the central, southwestern, and southeastern parts, particularly in the states of Assam, Tripura, and Manipur as shown in Fig. 5(c). In contrast, very low (16.17%) and low (32.50%) deforestation susceptibility zones were observed in the northern, southern, western, and some clustered locations of the study area, particularly in Mizoram, Arunachal Pradesh, Meghalaya, and Nagaland.

Deforestation susceptibility analysis using the EDAS model The EDAS model was successfully applied to demarcate the deforestation susceptibility zones. The model's outcome was classified into five different categories: very low (0.13–0.42), low (0.43–0.51), moderate (0.52–0.59), high (0.6–0.7), and very high (0.71–0.96) as shown in Fig. 5(b). The delineated deforestation susceptibility map revealed substantial variations in the deforestation potential of the study area. Approximately 15.33% of the region's area was very highly susceptible to deforestation, particularly in the states of Assam, Tripura, and Manipur. The map further demarcated approximately 14.68% of the study area as semi-critical in terms of deforestation susceptibility. Nevertheless, about 35.16%, 24.63%, and 10.20% of the study area were identified as having moderate, low, and very low deforestation susceptibility, respectively. The states such as Mizoram, Arunachal Pradesh, and Meghalaya exhibited moderate to very low deforestation susceptibility.

Deforestation susceptibility analysis using the WASPAS model Deforestation susceptibility zones were assigned using the Weighted Aggregated Sum Product Assessment (WASPAS), one

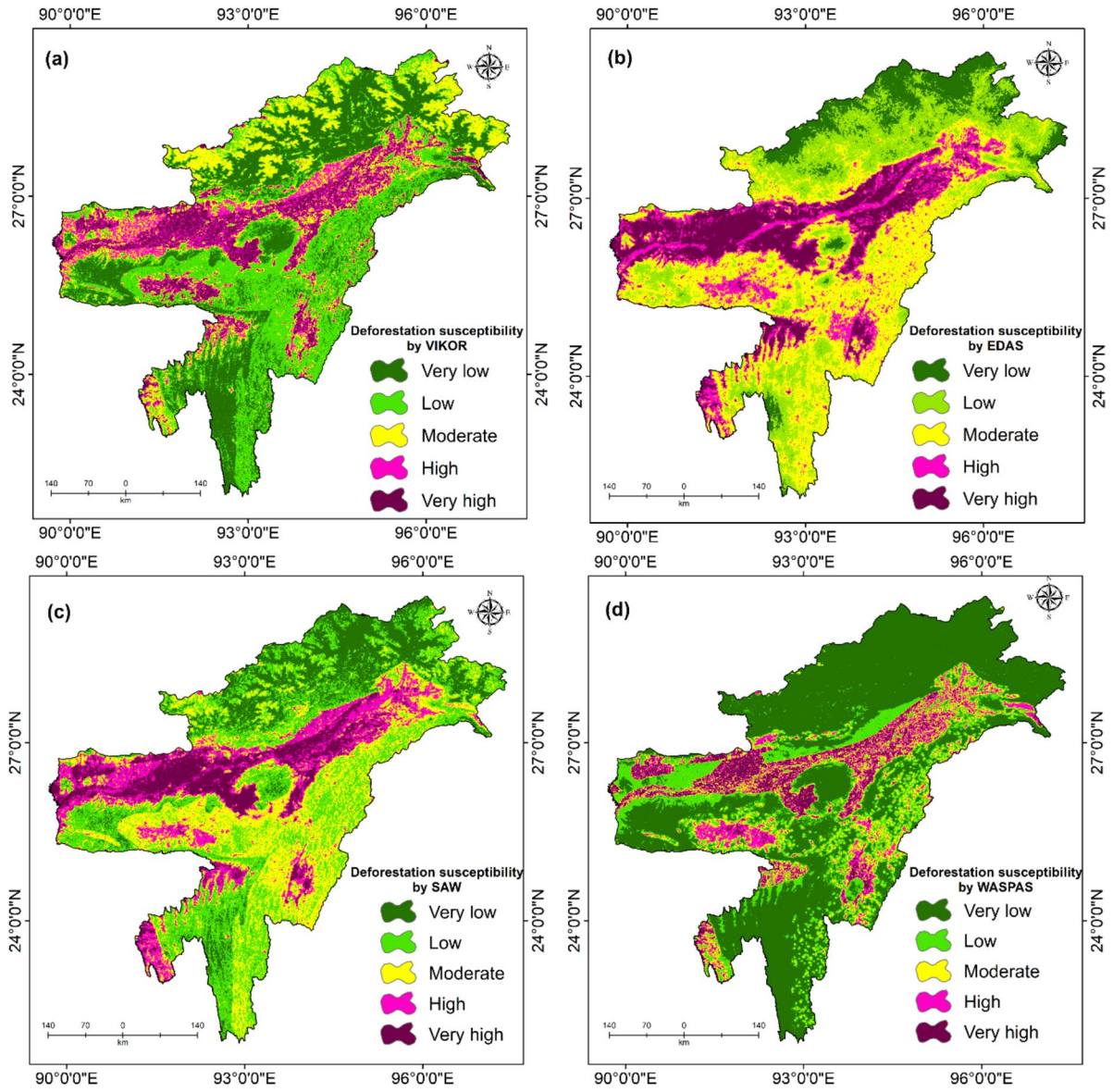

Fig. 5 Deforestation susceptibility maps using (**a**) VIKOR, (**b**) EDAS, (**c**) SAW, and (**d**) WASPAS

Table 6 Area and proportion area of deforestation susceptibility zones derived by different methods

Deforestation susceptibility	VIKOR		SAW		EDAS		WASPAS	
	Area (km^2)	Area (%)	Area (km^2)	Area (%)	Area (km^2)	Area (%)	Area (km^2)	Area (%)
Very low	71,671.45	28.28	40,979.16	16.17	25,857.79	10.20	137,478.11	54.25
Low	82,529.16	32.57	82,356.35	32.50	62,411.08	24.63	48,913.92	19.30
Medium	47,106.17	18.59	67,227.17	26.53	89,085.62	35.16	27,692.15	10.93
High	29,900.05	11.80	35,067.80	13.84	37,206.49	14.68	22,935.41	9.05
Very high	22,186.81	8.76	27,763.19	10.96	38,832.67	15.33	16,374.06	6.46

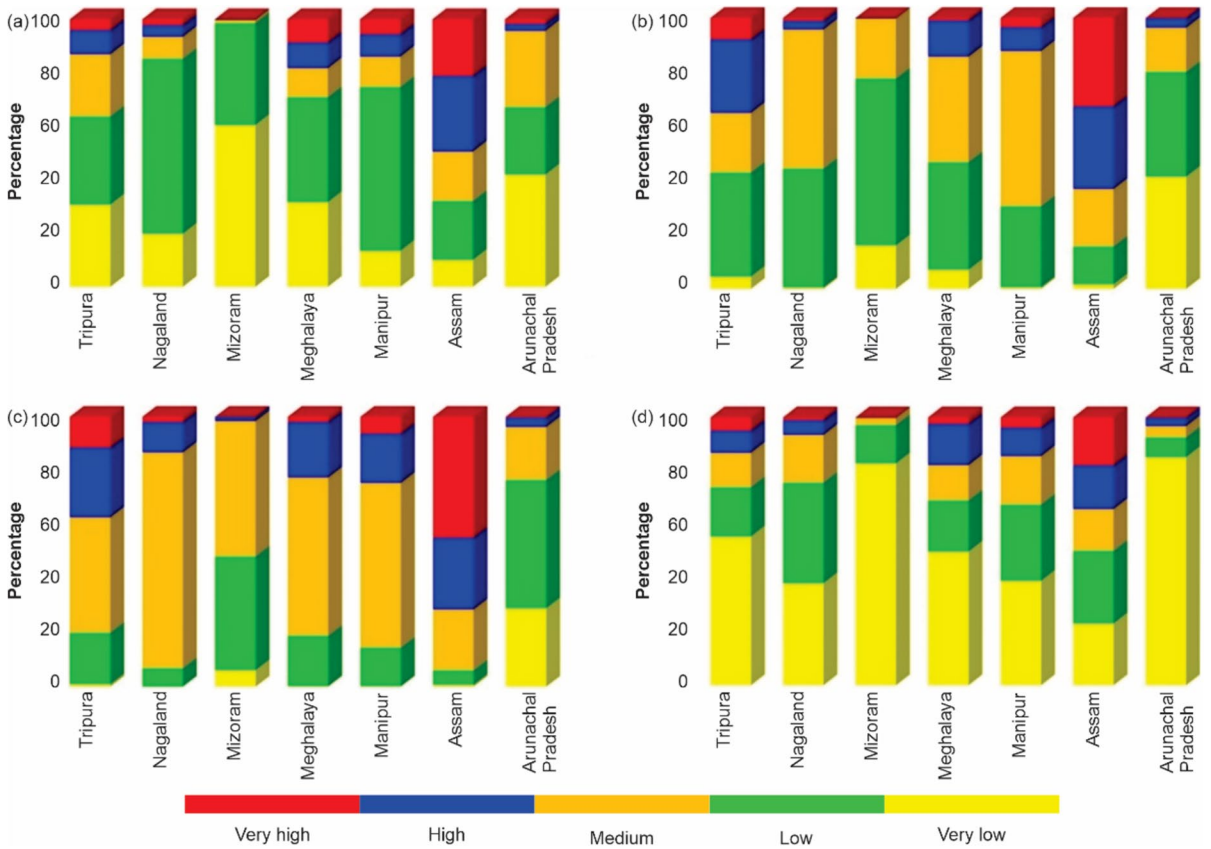

Fig. 6 Composite graph showing the distribution of area by deforestation susceptibility category, derived from different models for the seven states of Northeast India (in %): (**a**) VIKOR, (**b**) SAW, (**c**) EDAS, and (**d**) WASPAS models

of the most widely used MCDA models. The prediction result of the WASPAS model was classified into five different classes: very low (0.12–0.25), low (0.26–0.32), moderate (0.33–0.4), high (0.41–0.49), and very high (0.5–0.71) using the Janke natural breaks classifier technique. Most susceptibility zones fell within the very low and low susceptibility classes (137,478.11 km^2 and 48,913.92 km^2) compared to the high potential class (16,374.06 km^2). The spatial distribution of the "very high" to "very low" deforestation susceptibility zones showed areas covered by 6.46%, 9.05%, 10.93%, 19.30%, and 54.25%, respectively. From this model, it was found that states like Assam, Tripura, and Manipur are most vulnerable to deforestation. In contrast, states like Mizoram, Arunachal Pradesh, and Nagaland are less prone to deforestation (Fig. 5d).

Correlation studies of the models

Correlation analyses between the models (VIKOR-SAW, VIKOR-EDAS, VIKOR-WASPAS, SAW-EDAS, SAW-WASPAS, WASPAS-EDAS) were performed to identify the inter-relationships between them. Based on R^2 statistical measures, it was observed that a high positive correlation (R^2=0.8483) persisted among the EDAS-SAW techniques. VIKOR-SAW (R^2=0.7906) and SAW-WASPAS (R^2=0.7514) also exhibited a high positive correlation. Interestingly, VIKOR-WASPAS (R^2=0.7822) showed a high negative correlation. These results reflect the consistency of the normalization and aggregation outcomes among these four methods, adding to the dependability of the models. In contrast, EDAS-WASPAS and VIKOR-EDAS revealed a moderate and good correlation, i.e., R^2=0.6122 and R^2=0.5415, respectively. The graphical representation of these correlations is illustrated in Fig. 7.

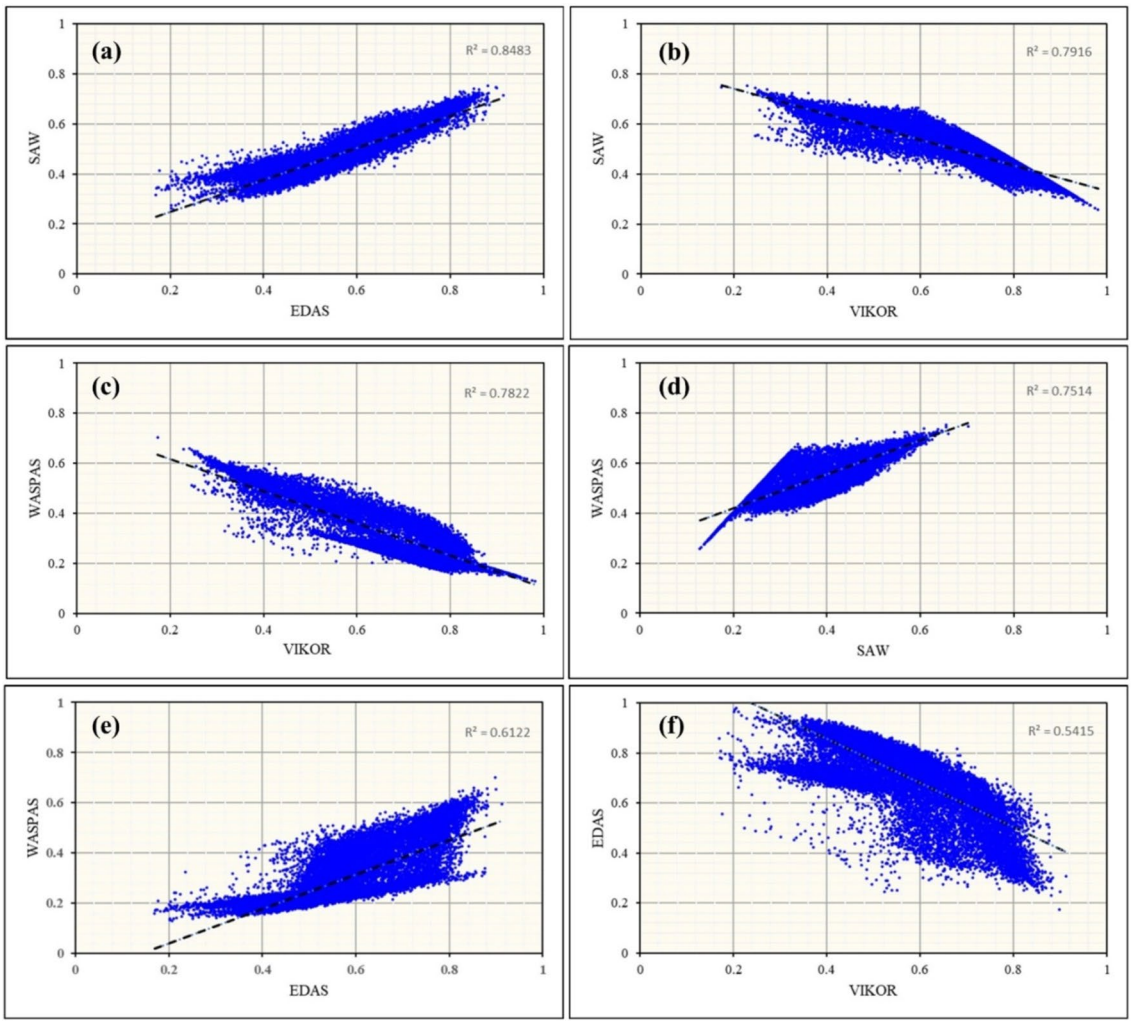

Fig. 7 Correlation studies of (**a**) SAW-EDAS, (**b**) SAW-VIKOR, (**c**) WASPAS-VIKOR, (**d**) WASPAS-SAW, (**e**) WASPAS-EDAS, (**f**) EDAS-VIKOR

Model validation

The statistical methods employed to analyze the acceptability of the model outputs are shown in Table 7. Among the methods used, VIKOR demonstrated better performance than the other three methods (SAW, EDAS, and WASPAS). The AUC of the receiver operating characteristics (ROC) values for VIKOR, SAW, EDAS, and WASPAS were 0.938, 0.901, 0.895, and 0.864, respectively. The Boolean ROC plot (Fig. 8) provided a visual validation of our models, indicating that the overall accuracy of the models ranges between 85 and 95%. This result signifies the good to very good predictive capability of these models for future prediction of deforestation susceptibility. The Cohen's kappa index values for these four methods were 0.830, 0.796, 0.783, and 0.768, respectively. This implies that the acceptability of these models in predicting deforestation is very promising, with VIKOR providing the best results.

The efficiency (E) values of these methods were 0.866, 0.824, 0.807, and 0.819, respectively. This finding demonstrated very good to excellent predictability of these four models. Moreover, the SAW method achieved the highest F-score value (0.829) among all the methods. The VIKOR model also had the highest sensitivity or True Positive Rate (TPR), with a value of 0.878, followed by SAW (0.821),

Table 7 Performance metrics of the four models (VIKOR, SAW, EDAS, WASPAS)

Metrics	VIKOR	SAW	EDAS	WASPAS
AUC	0.938	0.901	0.895	0.864
True positive rate (TPR)	0.878	0.821	0.819	0.802
False positive rate (FPR)	0.146	0.173	0.205	0.161
Cohen's kappa index	0.830	0.796	0.783	0.768
Accuracy or Efficiency (E)	0.866	0.824	0.807	0.819
True negative rate (TNR)	0.854	0.827	0.795	0.839
Miss rate	0.122	0.179	0.181	0.198
Positive predictive value (PPV)	0.856	0.837	0.798	0.856
False discovery rate (FDR)	0.144	0.163	0.202	0.144
Negative predictive value (NPV)	0.876	0.810	0.816	0.780
False omission rate (ROF)	0.124	0.190	0.184	0.220
F-score	0.771	0.829	0.808	0.828
Matthew's correlation coefficient (MCC)	0.586	0.647	0.614	0.638
Yule's Q	0.887	0.912	0.892	0.909
True skill statistics (TSS)	0.732	0.647	0.614	0.641

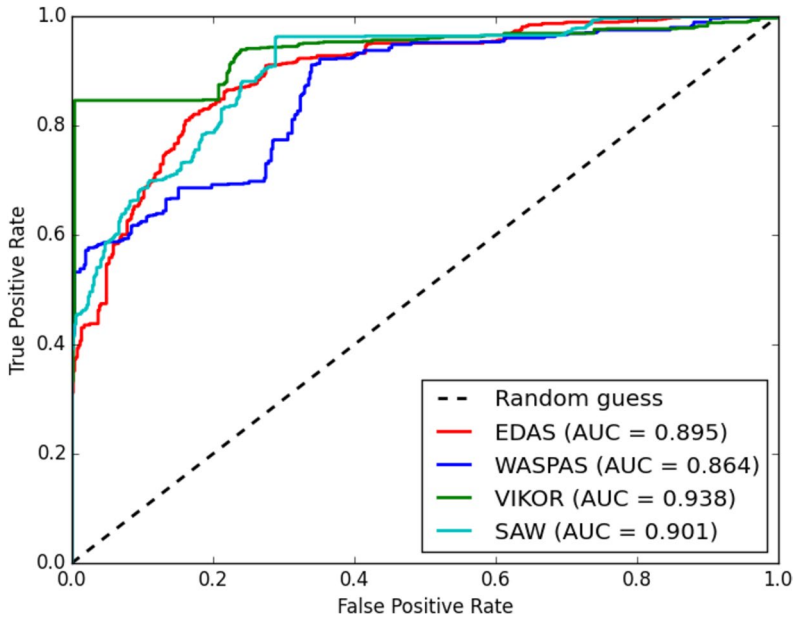

Fig. 8 ROC curves for validating the deforestation susceptibility maps

EDAS (0.819), and WASPAS (0.802). The specificity or False Positive Rate (FPR) values of these models were 0.146, 0.173, 0.205, and 0.161, respectively.

In this study, sensitivity analysis was conducted extensively across all relevant factors, including environmental, economic, and social criteria. The analysis revealed that certain environmental factors, such as deforestation rates and pollution levels, were particularly sensitive and significantly influenced the model's outcomes under different weighting schemes. This insight led to a more cautious approach in assigning weights to these sensitive criteria, ensuring that the model remained robust under various plausible scenarios. These sensitivity analyses not only confirmed the reliability of the model under different conditions but also provided critical insights into which factors were most influential, thereby guiding decision-makers in focusing their attention and resources on the most impactful areas. This approach enhances the credibility and transparency of the decision-making process,

Table 8 Wilcoxon signed-rank test comparing different MCDA models for deforestation susceptibility assessment

Model comparison	Z value[a]	*p*-value	Significance
SAW—VIKOR	− 22.600[b]	< 0.05	Yes
EDAS—VIKOR	− 16.402[b]	< 0.05	Yes
WASPAS—VIKOR	− 4.168[c]	< 0.05	Yes
WASPAS—SAW	− 19.841[c]	< 0.05	Yes
EDAS—SAW	− 8.234[c]	< 0.05	Yes
WASPAS—EDAS	− 15.336[c]	< 0.05	Yes

a = Wilcoxon signed ranks test; b = Based on negative ranks; c = Based on positive ranks

providing stakeholders with confidence in the robustness and adaptability of the model. Furthermore, the Wilcoxon signed-rank test was performed to verify the statistical differences between the deforestation susceptibility models. The result of this test indicated that all pairwise comparative models were significantly different, with *p*-values < 0.05 and Z values > ± 1.96. The Wilcoxon Signed Ranks Test (Z values) and the significance levels (*p*-values) of the different deforestation susceptibility models are detailed in Table 8.

Discussion

Deforestation in india: MCDM models for prediction and policy

Currently, deforestation poses a significant challenge and should, therefore, be a primary concern for researchers, policymakers, administrators, and environmentalists globally. In India, climate change significantly contributes to deforestation, such as through increases in global temperatures, which cause water stress in forests, compromising tree growth and increasing the mortality of trees that are unable to adapt to higher temperatures (Li et al., 2016; Lodh & Haldar, 2024). Additionally, prolonged droughts and lightning events can promote the occurrence of wildfires (Mishra et al., 2024b) and the proliferation of pests and diseases that attack trees. These factors contribute to forest degradation, reducing biodiversity and affecting the ecosystem services that forests provide, such as climate regulation, soil conservation, and water purification (Das et al., 2024).

It should also be noted that anthropogenic actions, such as the expansion of agricultural areas, severely contribute to deforestation. However, in recent decades, the Indian government has implemented various forest protection policies. One such policy is the National Afforestation and Eco-Development Program (Pujar et al., 2022), which aims to preserve forest cover through reforestation and sustainable management, recognizing the rights of indigenous communities and promoting participatory conservation. Although these policies have achieved some successes, challenges persist. These include the need for increased funding, effective monitoring, and mitigation of climate impacts to ensure the sustainability of Indian forests (Malik et al., 2014).

This study aimed to identify areas of forest loss and regions vulnerable to deforestation in Northeast India. By examining drivers of forest cover change and deforestation susceptibility using MCDM models, the research supports ongoing conservation efforts. The use of MCDM models in deforestation prediction has emerged as an effective tool for assessing and managing environmental impacts across the globe. In this study, the utilized models incorporated various parameters and criteria, such as vegetation cover, land use, proximity to roads, and human settlements, into an analytical framework that aids in identifying areas more likely to undergo deforestation. By integrating geospatial data, MCDM models enabled the future simulation of deforestation and allowed for the analysis of deforestation drivers and land use changes. The use of MCDM models enables decision-makers to formulate public policies based on predictive deforestation scenarios to mitigate impacts caused by the loss of vegetation cover (Dohale et al., 2024). Moreover, these models provide a transparent and quantitative approach, facilitating the communication and understanding of the decisions made. However, it is crucial to consider the quality of input data and the uncertainty associated with the predictions made by the models. Continuous updating and validation of MCDM models are essential to ensure their effectiveness in environmental conservation and the sustainable management of forests.

Studying deforestation prediction in India is crucial due to its rich biodiversity and the environmental challenges it faces. With an extensive range of tropical forests and a growing population, India encounters significant pressures on its natural resources (Basu & Basu, 2023). Understanding deforestation patterns is essential to mitigate habitat loss, conserve threatened

species, and protect vital ecosystem services. Furthermore, predicting deforestation can inform more sustainable land use policies and practices, promoting a balance between economic development and environmental conservation in the context of rapid urbanization and industrialization (Saha et al., 2020). A study by Lele and Joshi (2009) reported that the deforestation rate in Northeast India from 1972 to 1999 accounted for about 97,875 km^2, altering 30% of the forest cover in each state within the region. According to Hazarika and Bhattacharjee (2023), the maximum forest loss occurred in Nagaland, which aligns with the findings of this study. A quantitative assessment of forest loss in Northeast India from 2001 to 2021 was conducted using HGFC data, yielding significant findings. The analysis indicates that approximately one-tenth of the total forest area diminished over the last two decades in Northeast India. During this period, the highest forest loss in terms of forest coverage area occurred in Nagaland (23.44%), with more than 15% of forest cover lost in Mizoram and Tripura. According to data from the Forest Survey of India (2021), the highest forest loss between 2011 and 2021 occurred in Mizoram, followed by Nagaland. Assuming the accuracy of both this study and the Forest Survey of India, the discrepancy in findings—Mizoram showing the highest forest loss for the 2011–2021 period, while Nagaland ranks highest for 2001–2021 in this study—could be attributed to the differences in the time frames analyzed.

This analysis reveals that major forest loss in Mizoram occurred between 2015–2018. This trend aligns with the analysis of the Global Forest Watch (2024), which observed major forest loss during the same period. Deforestation potential mapping can serve as a crucial tool for preventing future deforestation and creating a roadmap (Bhutia et al., 2024). The incorporation of geospatial techniques and robust statistical methods makes the model more realistic and scientific. Consequently, a few statistical probabilistic methods and techniques have been implemented worldwide for spatial prediction of deforestation (Bera et al., 2022; Gayen & Saha, 2018).

Recently, machine learning techniques have also been applied in various types of prediction models. Deforestation susceptibility analysis using MCDM methods has been extensively employed. MCDM has proven to be a reliable approach for analyzing forest loss and facilitating the implementation of sustainable forest management.

The deforestation susceptibility zonation maps were prepared using the MCDM analysis method with a total of 20 explanatory factors. The object-based CRITIC statistical method was subsequently applied to calculate the weights of each parameter. Multicollinearity analysis was performed to avoid multicollinearity issues among these variables. In this paper, we employed the MCDM analysis methods VIKOR, SAW, EDAS, and WASPAS to assess deforestation susceptibility. Among these MCDM methods, the VIKOR method demonstrated better performance than the others during the validation of all four models, as explained in the previous results section. In many analyses using MCDM methods, the VIKOR model has proven to be more reliable. For instance, in a study in the Tarai region of the Himalayas, MCDM analysis methods AHP, TOPSIS, and VIKOR were used to assess deforestation susceptibility. Among all these methods, the VIKOR model emerged as the most reliable (Bera et al., 2022). During a study of forest fire susceptibility in Turkey, all three methods used—TOPSIS, AHP, and VIKOR—were found to be highly accurate, with accuracy levels of 85% to 90%, making them useful for analyzing forest fire susceptibility (Sari, 2021). In another study in the sub-Himalayan region of northern West Bengal, GIS and three MCDM methods, TOPSIS, VIKOR, and EDAS, were used to analyze areas of flood susceptibility. During this analysis, both TOPSIS and VIKOR methods were found to be reliable (Mitra & Das, 2022). In yet another study in the Murshidabad district of West Bengal, aimed at preparing a groundwater susceptibility map, the VIKOR model was highly efficient among the three MCDM methods used in the study—TOPSIS, VIKOR, and EDAS (Paul & Roy, 2024). Therefore, the reliability of the VIKOR method during susceptibility analysis in different areas has been well demonstrated, and our analysis also shows VIKOR to be a more accurate and reliable method.

According to our study, the susceptibility maps prepared using the VIKOR model indicate that Assam, Tripura, and Arunachal Pradesh are highly susceptible to deforestation. Deforestation is influenced by factors such as altitude, slope, slope aspect, and distance from roads, settlements, rivers, and forest edges (Gayen & Saha, 2018). With the significant presence of the Brahmaputra River and easier access to forest edges by road in Assam, the forest areas of

Assam could be highly susceptible to deforestation. The forest areas in Arunachal Pradesh are particularly vulnerable to climate change. According to the climate change exposure hotspot map of forest cover in 2030, prepared by the Forest Survey of India (2021), which takes into account the combined changes in temperature and precipitation, the northern part of Arunachal Pradesh is highly vulnerable to climate change (Forest Survey of India, 2021). The Forest Survey of India (2021) report also highlighted that the major forest areas of Mizoram, Nagaland, Manipur, Meghalaya, and Tripura experienced frequent forest fires in 2020–2021, which could contribute to forest loss. Shifting cultivation (Jhum) is widespread among the tribes living in the hilly terrains of the northeastern states, constituting about 86 percent of the region's total cultivated area (Haokip et al., 2021). The slash-and-burn practices of the prevalent shifting (Jhum) cultivation in the northeast region are a major factor in the loss of forest areas in northeastern India. This was identified as a significant cause of forest loss during 2017–2019, according to the Forest Survey of India, 2021).

Limitations and future scopes: Measures to minimize deforestation and protect remaining forest areas

While the study is impactful, it faces some limitations due to the nature of the adopted methodology. The 'CRITIC' model, an objective weighting approach, does not incorporate expert opinions or field observations, which may introduce potential errors. Since this method is newly applied in deforestation susceptibility assessment, it lacks comparative analysis with previous studies. Additionally, several key factors driving deforestation, such as shifting cultivation and forest fires, were not addressed in this study. Furthermore, the HGFC method only collects data on trees taller than 5 m, thus neglecting smaller trees.

Despite these research processes and hypothesis limitations, the study's results are valid and scientifically sound, suitable for adoption in future studies in regions with similar geo-environmental conditions. For future research, hybrid MCDM models such as E-VIKOR (Entropy-VIKOR), E-EDAS (EntropyEDAS), E-SAW (Entropy-SAW), E-WASPAS (Entropy-WASPAS), AHP-VIKOR, AHP-SAW, etc. can be applied. Additionally, various ensemble machine learning algorithms (REPTree, MLP-bagging, MLP-dagging, MLPnn, etc.) can be used to determine deforestation susceptibility zones in this region.

The study emphasized the need for a multifaceted approach that combines regulatory, technological, and community-based strategies to effectively address the challenges of deforestation in the Northeast region of India. These recommended measures were developed in consultation with local stakeholders, environmental experts, and policymakers to ensure their relevance and feasibility. Not only do these strategies aim to curb deforestation, but they also seek to enhance the resilience of forest ecosystems and the communities that depend on them. Based on the research findings focused on deforestation dynamics in the Northeast region of India, it is imperative to implement specific measures aimed at minimizing deforestation and protecting the remaining forest areas. The recommendations outlined below are derived from a comprehensive analysis of the drivers, patterns, and impacts of deforestation observed in the region, supplemented by a rigorous evaluation of potential conservation strategies. We propose the following recommendations to minimize deforestation and protect forests:

1. Strengthening Regulatory Frameworks: Enhance the enforcement of existing forestry laws and policies while revising them to address current gaps and inefficiencies. Implement stricter controls on illegal logging and land conversion activities, and introduce incentives for compliance with forest conservation efforts.
2. Community-Based Forest Management (CBFM): Empower local communities through CBFM programs that include them in the decision-making process for forest management. Provide training and resources to help communities engage in sustainable forestry practices, which can lead to improved forest stewardship and economic benefits from forest resources.
3. Afforestation and Reforestation Programs: Initiate large-scale afforestation and reforestation projects to restore degraded forest lands. Utilize native species to ensure ecological compatibility and resilience, and tailor tree planting efforts to local climate and soil conditions to enhance survival rates.
4. Use of Technology in Monitoring and Enforcement: Leverage advanced technologies such as

remote sensing, drones, and GIS for real-time monitoring of forest cover changes. These tools can aid in the early detection of illegal activities and facilitate prompt enforcement actions.

5. Promotion of Alternative Livelihoods: Develop and promote alternative livelihood options for communities reliant on deforestation-prone activities. This strategy can include agroforestry, ecotourism, and other sustainable agricultural practices that provide economic benefits without depleting forest resources.
6. Education and Awareness Programs: Implement comprehensive education and awareness campaigns to inform the public about the importance of forests and the adverse impacts of deforestation. Educational programs should target schools, local communities, and stakeholders involved in land-use decisions.
7. Strengthening Biodiversity Conservation Initiatives: Integrate biodiversity conservation into forest management plans. Establish and expand protected areas, particularly in biodiversity hotspots, to conserve critical habitats and endangered species.
8. Collaborative Research and International Cooperation: Foster collaborative research on sustainable forestry and conservation techniques between local universities, international organizations, and government agencies. Encourage participation in international forestry conservation programs to exchange knowledge and resources.
9. Policy Integration and Multisectoral Coordination: Ensure that forest conservation measures are integrated into broader land-use, agricultural, and developmental policies. Establish coordination mechanisms among various governmental and non-governmental entities to align efforts and optimize resource utilization.

Conclusions

This study evaluated deforestation susceptibility zones from 2001 to 2021 in the Seven Sister States of Northeast India. Key findings indicate a substantial decline in forest cover, with the region experiencing an average forest loss of 10.49% over two decades. Arunachal Pradesh had the highest initial forest cover in 2000, while Tripura had the lowest. Mizoram exhibited the highest percentage of forest cover relative to its geographical area. The study reveals that Nagaland experienced the greatest percentage loss of forest cover, whereas Arunachal Pradesh had the least relative loss. Additionally, Assam displayed the highest mean annual deforestation rate, whereas Tripura had the lowest.

The research also utilized multiple deforestation susceptibility models (VIKOR, SAW, EDAS, and WASPAS) to categorize the regions based on their vulnerability to deforestation. The models produced varying results; VIKOR identified Assam, Tripura, and Arunachal Pradesh as highly susceptible to deforestation, while Mizoram, Nagaland, and Manipur were categorized as less vulnerable. Model validation through ROC and Cohen's kappa indices highlighted VIKOR as the most reliable method, demonstrating good to very good predictive capability across the board.

The data analysis directly correlates with the conclusions drawn regarding the varying degrees of deforestation susceptibility among the states. For instance, the VIKOR model's categorization of Assam, Tripura, and Arunachal Pradesh as highly susceptible aligns with the observed high mean annual forest loss in these states. The significant forest loss recorded in Nagaland (23.44%) compared to the lower loss in Arunachal Pradesh (4.20%) is consistent with their susceptibility classifications from the models. The discrepancies in susceptibility identified by the different models underscore the importance of selecting appropriate methods for accurate deforestation risk assessment, as reflected in the significant performance differences among the models.

The findings of this study have several implications for forest conservation and policy-making. The high susceptibility to deforestation in states like Assam and Tripura suggests an urgent need for targeted conservation efforts and stricter forest management policies in these regions. The results indicate that conservation strategies should be tailored to the specific deforestation risks of each state, considering the varying levels of susceptibility. Policymakers should consider enhancing forest protection measures, promoting sustainable land-use practices, and increasing community involvement in conservation efforts. The high performance of the VIKOR model in predicting deforestation susceptibility suggests that it could be a valuable tool for guiding policy decisions and resource allocation.

This study makes a significant contribution to the field of forest management and deforestation analysis by providing a comprehensive evaluation of forest cover dynamics and susceptibility to deforestation in Northeast India. By employing multiple deforestation susceptibility models and validating their results, the research offers a nuanced understanding of regional variations in deforestation risk. The study enhances the existing knowledge base on forest loss patterns and susceptibility, providing a valuable reference for future research and policy development. The detailed analysis of model performance and susceptibility mapping also contributes to improving the methodologies used in deforestation studies. The findings of this study can provide valuable insights for policymakers, government representatives, and forest officials, guiding them in taking effective measures for deforestation management and promoting environmental sustainability in these regions of Northeast India.

Author contribution R.G.: Conceptualization; Data curation; Formal analysis; Methodology; Writing—review & editing. M.M.: Conceptualization; Data curation; Formal analysis; Methodology; Writing—review & editing. B.B.: Conceptualization; Data curation; Formal analysis; Methodology; Writing—review & editing. S.G.: Supervision; Writing—review & editing. C.A.G.S.: Visualization; and Writing—review & editing. R.M.S.: Visualization; and Writing—review & editing. K.D.O.B.: Investigation; and Writing—original draft.

Funding No funding was received.

Data availability Data will be made available on reasonable request.

Declarations

Ethical approval All authors have read, understood, and have complied as applicable with the statement on "Ethical responsibilities of Authors."

Competing interests The authors declare no competing interests.

Disclosure statement No potential conflict of interest was reported by the authors.

References

Abugre, S., & Sackey, E. K. (2022). Diagnosis of perception of drivers of deforestation using the partial least squares path modeling approach. *Trees, Forests and People, 8*, 100246. https://doi.org/10.1016/j.tfp.2022.100246

Ali, A. I., & Das, I. (2003). Tribal Situation in North East India. *Studies of Tribes and Tribals, 1*(2), 141–148. https://doi.org/10.1080/0972639X.2003.11886492

Altarez, R. D. D., Apan, A., & Maraseni, T. (2023). Deep learning U-Net classification of Sentinel-1 and 2 fusions effectively demarcates tropical montane forest's deforestation. *Remote Sensing Applications: Society and Environment, 29*, 100887. https://doi.org/10.1016/j.rsase.2022.100887

Ameri, A. A., Pourghasemi, H. R., & Cerda, A. (2018). Erodibility prioritization of sub-watersheds using morphometric parameters analysis and its mapping: A comparison among TOPSIS, VIKOR, SAW, and CF multi-criteria decision making models. *Science of the Total Environment, 613–614*, 1385–1400. https://doi.org/10.1016/j.scitotenv.2017.09.210

Arabameri, A., Saha, S., Chen, W., Roy, J., Pradhan, B., & Bui, D. T. (2020). Flash flood susceptibility modelling using functional tree and hybrid ensemble techniques. *Journal of Hydrology, 587*, 125007. https://doi.org/10.1016/j.jhydrol.2020.125007

Babu, S. V. (2014). Clearing the Forest: Colonialism and Deforestation in Nagaland, Northeast India. *IOSR Journal of Humanities and Social Science, 19*(6), 14–16. https://doi.org/10.9790/0837-19651416

Bajaj, J. K. (2011). Scheduled *Tribes of India: Religious demography and representation*. Chennai: Centre for Policy Studies. pp. 50.

Basu, A., & Basu, J. P. (2023). Impact of forest governance and enforcement on deforestation and forest degradation at the district level: A study in West Bengal State India. *Regional Sustainability, 4*(4), 441–452. https://doi.org/10.1016/j.regsus.2023.11.002

Bax, V., & Francesconi, W. (2018). Environmental predictors of forest change: An analysis of natural predisposition to deforestation in the tropical Andes region, Peru. *Applied Geography, 91*, 99–110. https://doi.org/10.1016/j.apgeog.2018.01.002

Bera, B., Saha, S., & Bhattacharjee, S. (2020). Forest cover dynamics (1998 to 2019) and prediction of deforestation probability using binary logistic regression (BLR) model of Silabati watershed, India. *Trees, Forests and People, 2*, 100034. https://doi.org/10.1016/j.tfp.2020.100034

Bera, B., Shit, P. K., Sengupta, N., Saha, S., & Bhattacharjee, S. (2022). Susceptibility of deforestation hotspots in Terai-Dooars belt of Himalayan Foothills: A comparative analysis of VIKOR and TOPSIS models. *Journal of King Saud University - Computer and Information Sciences, 34*(10), 8794–8806. https://doi.org/10.1016/j.jksuci.2021.10.005

Bhattacharya, R. K., Chatterjee, N. D., & Das, K. (2020). Sub-basin prioritization for assessment of soil erosion susceptibility in Kangsabati, a plateau basin: A comparison between MCDM and SWAT models. *Science of the Total Environment, 734*, 139474. https://doi.org/10.1016/j.scitotenv.2020.139474

Bhutia, K. D., Mishra, M., Guria, R., Baraj, B., Naik, A. K., da Silva, R. M., TV, Nascimento, C. A., & Santos. (2024). Evaluation of large-scale deforestation susceptibility mapping in the mountainous region of the Himalayas: A case study of the Khangchendzonga Biosphere Reserve, India.

Remote Sensing Applications: Society and Environment, 36, 101285. https://doi.org/10.1016/j.rsase.2024.101285

Census of India (2011). *Districts of Uttar Pradesh*. Retrieved September 9, 2024, from https://censusindia.gov.in

Chen, S., Woodcock, C., Dong, L., Tarrio, K., Mohammadi, D., & Olofsson, P. (2024). Review of drivers of forest degradation and deforestation in Southeast Asia. *Remote Sensing Applications: Society and Environment, 33*, 101129. https://doi.org/10.1016/j.rsase.2023.101129

Chowdhuri, I., Pal, S. C., & Chakrabortty, R. (2020). Flood susceptibility mapping by ensemble evidential belief function and binomial logistic regression model on river basin of eastern India. *Advances in Space Research, 65*(5), 1466–1489. https://doi.org/10.1016/j.asr.2019.12.003

Da Silva, C. F. A., de Andrade, M. O., dos Santos, A. M., & de Melo, S. N. (2023a). Road network and deforestation of indigenous lands in the Brazilian Amazon. *Transportation Research Part d: Transport and Environment, 119*, 103735. https://doi.org/10.1016/j.trd.2023.103735

Dagar, J.C., Gupta, S.R., & Sileshi, G.W. (2023). Urban and Peri-Urban Agroforestry to Sustain Livelihood and Food Security in the Face of Global Environmental Change and Epidemic Threats. In: Dagar, J.C., Gupta, S.R., Sileshi, G.W. (eds) Agroforestry for Sustainable Intensification of Agriculture in Asia and Africa. *Sustainability Sciences in Asia and Africa*. Springer, Singapore. https://doi.org/10.1007/978-981-19-4602-8_4

U Das P Datta B Behera 2024 Identification of Major Threats of Climate Change, Hazards, and Anthropogenic Activities on Biodiversity Conservation in the Buxa Tiger Reserve Environmental Management. https://doi.org/10.1007/s00267-024-01998-y

Diakoulaki, D., Mavrotas, G., & Papayannakis, L. (1995). Determining objective weights in multiple criteria problems: The critic method. *Computers and Operations Research, 22*(7), 763–770. https://doi.org/10.1016/0305-0548(94)00059-H

Dohale, V., Kamble, S., Ambilkar, P., Gold, S., & Belhadi, A. (2024). An integrated MCDM-ML approach for predicting the carbon neutrality index in manufacturing supply chains. *Technological Forecasting and Social Change, 201*, 123243. https://doi.org/10.1016/j.techfore.2024.123243

Food and Agriculture Organization (2022). The State of the World's Forests 2022 Forest pathways for green recovery and building inclusive, resilient and sustainable economies Rome, FAO. https://doi.org/10.4060/cb9360en

Food and Agriculture Organization (2024). Forest resources assessment – processed by Our World in Data. Annual deforestation rate . UN Food and Agriculture Organization (FAO). Forest Resources Assessment

Forest Resources Assessment 2020 Global Forest Resources Assessment 2020 – Key findings Rome. https://doi.org/10.4060/ca8753en

Forest Survey of India (2021). India state of forest report 2017. Ministry of Environment and Forests, Government of India. Retrieved May 2, 2023, from http://fsi.nic.in/forest-report-2021

Galiatsatos, N., Donoghue, D., Watt, P., Bholanath, P., Pickering, J., Hansen, M., & Mahmood, A. (2020). An Assessment of Global Forest Change Datasets for National Forest Monitoring and Reporting. *Remote Sensing, 12*, 1790. https://doi.org/10.3390/rs12111790

Gayen, A., & Saha, S. (2018). Deforestation probable area predicted by logistic regression in Pathro river basin: A tributary of Ajay river. *Spatial Information Research, 26*(1), 1–9. https://doi.org/10.1007/s41324-017-0151-1

Ghorabaee, M. K., Amiri, M., Sadaghiani, J. S., & Zavadskas, E. K. (2015a). Multi-Criteria Project Selection Using an Extended VIKOR Method with Interval Type-2 Fuzzy Sets. *International Journal of Information Technology and Decision Making, 14*, 993–1016. https://doi.org/10.1142/S0219622015500212

Ghorabaee, M. K., Zavadskas, E. K., Olfat, L., & Turskis, Z. (2015). Multi-Criteria Inventory Classification Using a New Method of Evaluation Based on Distance from Average Solution (EDAS). *Informatica, 26*(3), 435–451.

Giri, K., Mishra, G., Rawat, M., Pandey, S., Bhattacharyya, R., Bora, N., & Rai, J.P.N. (2020). Traditional Farming Systems and Agro-biodiversity in Eastern Himalayan Region of India. In: Goel R., Soni R., Suyal D. (eds) Microbiological Advancements for Higher Altitude Agro-Ecosystems & Sustainability. *Rhizosphere Biology*. Springer, Singapore. https://doi.org/10.1007/978-981-15-1902-4_5

Global Forest Watch (2024). *Forest monitoring designed for action*. Retrieved September 11, 2024, from https://www.globalforestwatch.org/dashboards

Guria, R., Mishra, M., da Silva, R. M., Mishra, M., & Santos, C. A. G. (2024a). Predicting forest fire probability in Simlipal Biosphere Reserve (India) using Sentinel-2 MSI data and machine learning. *Remote Sensing Applications: Society and Environment, 36*, 101311. https://doi.org/10.1016/j.rsase.2024.101311

Guria, R., Mishra, M., Dutta, S., da Silva, R. M., & Santos, C. A. G. (2024b). Remote sensing, GIS, and analytic hierarchy process-based delineation and sustainable management of potential groundwater zones: A case study of Jhargram district, West Bengal India. *Environmental Monitoring and Assessment, 196*(1), 95. https://doi.org/10.1007/s10661-023-12205-6

Hansen, M. C., Potapov, P. V., Moore, R., Hancher, M., Turubanova, S. A., Tyukavina, A., Thau, D., Stehman, S. V., Goetz, S. J., Loveland, T. R., Kommareddy, A., Egorov, A., Chini, L., Justice, C. O., & Townshend, J. R. G. (2013). High-Resolution Global Maps of 21st-Century Forest Cover Change. *Science*, 342 (15 November): 850–53

Haokip, I., Devi, M., Das, H., Dey, P., Kumar, D., & Tasung, A. (2021). Shifting cultivation in northeast India: Sustainability issues and strategies for improvement. *Soil Health Management: Knowledge, 4*(2), 3–6.

Hazarika, B., & Bhattacharjee, N. (2023). Population pressure and its impact on forest resources in North East India. *Journal of Applied School Psychology* 4245–4255.

Hosseini, S., Amirnejad, H., & Azadi, H. (2024). Impacts of Hyrcanian forest ecosystem loss: The case of Northern Iran. *Environment, Development and Sustainability*. https://doi.org/10.1007/s10668-023-04408-1

Hwang, C-L., & Masud, A. S. M. (2012). Multiple objective decision making-methods and applications: a state-of-the-art survey. 164. *Springer Science & Business Media*, 2012.

Islam, N., Sarkar, B., Basak, A., Das, P., Paul, I., Debnath, M., & Roy, R. (2022). A novel GIS-based MCDM approach to identify the potential eco-tourism sites in the Eastern Dooars region (Himalayan foothill) of West Bengal India. *Geocarto International, 37*(26), 13145–13175. https://doi.org/10.1080/10106049.2022.2076917

Kayet, N., Pathak, K., Kumar, S., Singh, C. P., Chowdary, V. M., Chakrabarty, A., Sinha, N., Shaik, I., & Ghosh, A. (2021). Deforestation susceptibility assessment and prediction in hilltop mining-affected forest region. *Journal of Environmental Management, 289*, 112504. https://doi.org/10.1016/j.jenvman.2021.112504

Kumar, R., Nandy, S., Agarwal, R., & Kushwaha, S. P. S. (2014). Forest cover dynamics analysis and prediction modeling using logistic regression model. *Ecological Indicators, 45*, 444–455. https://doi.org/10.1016/j.ecolind.2014.05.003

Kumari, R., Banerjee, A.A., Kumar, R., Kumar, A., Saikia, P., & Khan, M.L. (2019). Deforestation in India: Consequences and Sustainable Solutions. *Forest Degradation Around the World*. 1–18. https://doi.org/10.5772/intechopen.85804

Lele, N., & Joshi, P. K. (2009). Analyzing deforestation rates, spatial forest cover changes and identifying critical areas of forest cover changes in North-East India during 1972–1999. *Environmental Monitoring and Assessment, 156*(1–4), 159–170. https://doi.org/10.1007/s10661-008-0472-6

Li, Y., Zhao, M., Mildrexler, D. J., Motesharrei, S., Mu, Q., Kalnay, E., Zhao, F., Li, S., & Wang, K. (2016). Potential and actual impacts of deforestation and afforestation on land surface temperature. *Journal of Geophysical Research: Atmospheres, 121*, 14372–14386. https://doi.org/10.1002/2016JD024969

Lodh, A., & Haldar, S. (2024). Investigating the impact of tropical deforestation on Indian monsoon hydro-climate: A novel study using a regional climate model. *Natural Hazards*. https://doi.org/10.1007/s11069-024-06615-z

Malik, Z. A., Bhat, J. A., & Bhatt, A. B. (2014). Forest resource use pattern in Kedarnath wildlife sanctuary and its fringe areas (a case study from Western Himalaya, India). *Energy Policy, 67*, 138–145. https://doi.org/10.1016/j.enpol.2013.12.016

Mandal, R. K. (2011). Changing agricultural scenario and its impact on food habit in north east states of India. *Food Biology, 1*(1), 14–21.

Mishra, G., & Francaviglia, R. (2021). Land uses, altitude and texture effects on soil parameters A comparative study in two districts of Nagaland Northeast India. *Agriculture, 11*(2), 1–14. https://doi.org/10.3390/agriculture11020171

Mishra, M., Guria, R., Baraj, B., Nanda, A. P., Santos, C. A. G., da Silva, R. M., & Laksono, F. A. T. (2024). Spatial analysis and machine learning prediction of forest fire susceptibility: A comprehensive approach for effective management and mitigation. *Science of the Total Environment, 926*, 171713. https://doi.org/10.1016/j.scitotenv.2024.171713

Mishra, M., Santos, C. A. G., Nascimento, T. V. M. do, Dash, M. K., Silva, R. M. da, Kar, D., & Acharyya, T. 2022 Mining impacts on forest cover change in a tropical forest using remote sensing and spatial information from 2001–2019: A case study of Odisha (India). Journal of Environmental Management 302 114067

Mishra, M., Acharyya, T., Guria, R., Rout, N. R., Santos, C. A. G., da Silva, R. M., Srivastava, S., Kumari, R., & Pradhan, A. K. (2024b). Lightning-related fatalities in India (1967–2020): a detailed overview of patterns and trends. *Environment, Development and Sustainability*, 1–30. https://doi.org/10.1007/s10668-024-05276-z

Mitra, R., & Das, J. (2022). A comparative assessment of food susceptibility modelling of GIS-based TOPSIS, VIKOR, and EDAS techniques in the Sub-Himalayan foothills region of Eastern India. *Environmental Science and Pollution Research, 30*, 16036–67. https://doi.org/10.1007/s11356-022-23168-5

Mo, L., Zohner, C. M., Reich, P. B., Liang, J., de Miguel, S., Nabuurs, G.-J., Renner, S. S., van den Hoogen, J., Araza, A., Herold, M., Mirzagholi, L., Ma, H., Averill, C., Phillips, O. L., Gamarra, J. G. P., Hordijk, I., Routh, D., Abegg, M., Yao, Y. C. A., … Crowther, T. W. (2023). Integrated global assessment of the natural forest carbon potential. *Nature, 624*, 92–101. https://doi.org/10.1038/s41586-023-06723-z

Murata, F., Hayashi, T., Matsumoto, J., & Asada, H. (2007). Rainfall on the Meghalaya plateau in northeastern India-one of the rainiest places in the world. *Natural Hazards, 42*(2), 391–399. https://doi.org/10.1007/s11069-006-9084-z

Nag, S. (2022). Vanishing Rains: Deforestation, Declining Rainfall, and Desiccation in North East India With Special Reference to Cherrapunji, the "Rainiest Spot on the Globe". In *Urban Development and Environmental History in Modern South Asia* (pp. 153–166). Routledge.

Opricovic, S. (1998). *Multicriteria Optimization of Civil Engineering Systems*, Faculty of Civil Engineering, Belgrade

Pandey, D. K., Momin, K. C., Dubey, S. K., & Adhiguru, P. (2022). Biodiversity in agricultural and food systems of jhum landscape in the West Garo Hills North-Eastern India. *Food Security, 14*, 791–804. https://doi.org/10.1007/s12571-021-01251-y

Paul, S., & Roy, D. (2024). Geospatial modeling and analysis of groundwater stress-prone areas using GIS-based TOPSIS, VIKOR, and EDAS techniques in Murshidabad district India. *Model Earth Systems and Environment, 10*, 121–141. https://doi.org/10.1007/s40808-022-01589-y

Paul, S., Das, T. K., Pharung, R., Ray, S., Mridha, N., Kalita, N., Ralte, V., Borthakur, S., Burman, R. R., Tripathi, A. K., & Singh, A. K. (2020). Development of an indicator based composite measure to assess livelihood sustainability of shifting cultivation dependent ethnic minorities in the disadvantageous Northeastern region of India. *Ecological Indicators, 110*, 105934. https://doi.org/10.1016/j.ecolind.2019.105934

Pujar, G. S., Pasha, S. V., Balaji, Y., Kalyandeep, K., Lesslie, A., Ravishankar, T., & Singh, R. P. (2022). National Assessment of Afforestation Activities in India, a Key SDG Target, Under the World's Largest Social Safety Scheme. *Journal of the Indian Society of Remote Sensing, 50*, 1423–1436. https://doi.org/10.1007/s12524-022-01536-5

Qi, J., Zhang, Y., Zhang, J., Chen, Y., Wu, C., Duan, C., Cheng, Z., & Pan, Z. (2022). Research on the Evaluation of Geological Environment Carrying Capacity Based on the AHP-CRITIC Empowerment Method. *Land, 11*(8), 1196. https://doi.org/10.3390/land11081196

Rasyid, A. R., Bhandary, N. P., & Yatabe, R. (2016). Performance of frequency ratio and logistic regression model in creating GIS based landslides susceptibility map at Lompobattang Mountain, Indonesia. *Geoenvironmental Disasters, 3*, 1–6. https://doi.org/10.1186/s40677-016-0053-x

Rawat, M. S., Zhimo, V. V., & Imchen, N. (2018). Deforestation in Nagaland, North-East India: Causes, Effects and Subsequent Environmental Degradation-A Preliminary Review. *Global Journal of Current Research., 6*(3), 61–70.

Rehman, S., & Azhoni, A. (2023). Analyzing landslide susceptibility, health vulnerability and risk using multi-criteria decision-making analysis in Arunachal Pradesh, India. *Acta Geophysica, 71*, 101–128. https://doi.org/10.1007/s11600-022-00943-z

Robbins Schug, G., Buikstra, J. E., DeWitte, S. N., Baker, B. J., Berger, E., Buzon, M. R., Davies-Barrett, A. M., Goldstein, L., Grauer, A. L., Gregoricka, L. A., & Halcrow, S. E. (2023). Climate change, human health, and resilience in the Holocene. *Proceedings of the National Academy of Sciences, 120*(4), e2209472120. https://doi.org/10.1073/pnas.2209472120

Saha, S., Saha, M., Mukherjee, K., Arabameri, A., Ngo, P. T. T., & Paul, G. C. (2020). Predicting the deforestation probability using the binary logistic regression, random forest, ensemble rotational forest, REPTree: A case study at the Gumani River Basin India. *Science of the Total Environment, 730*, 139197. https://doi.org/10.1016/j.scitotenv.2020.139197

Saha, S., Paul, G. C., Pradhan, B., Abdul Maulud, K. N., & Alamri, A. M. (2021). Integrating multilayer perceptron neural nets with hybrid ensemble classifiers for deforestation probability assessment in Eastern India. *Geomatics, Natural Hazards and Risk, 12*(1), 29–62. https://doi.org/10.1080/19475705.2020.1860139

Saha, S., Bhattacharjee, S., Shit, P. K., Sengupta, N., & Bera, B. (2022). Deforestation probability assessment using integrated machine learning algorithms of Eastern Himalayan foothills (India). *Resources, Conservation and Recycling Advances, 14*, 200077. https://doi.org/10.1016/j.rcradv.2022.200077

Sahana, M., Hong, H., Sajjad, H., Liu, J., & Zhu, A. X. (2018). Assessing deforestation susceptibility to forest ecosystem in Rudraprayag district, India using fragmentation approach and frequency ratio model. *Science of the Total Environment, 627*, 1264–1275. https://doi.org/10.1016/j.scitotenv.2018.01.290

Santos, C. A. G., T. V. M., Nascimento, R. M., & Silva. (2020). Analysis of forest cover changes and trends in the Brazilian semiarid region between 2000 and 2018. *Environmental Earth Sciences, 79*(18), 418. https://doi.org/10.1007/s12665-020-09158-1

Santos, J. Y. G., Montenegro, S. M. G. L., Silva, R. M., Santos, C. A. G., Quinn, N. W., Xavier, A. P. C., & Ribeiro Neto, A. (2021). Modeling the impacts of future LULC and climate change on runoff and sediment yield in a strategic basin in the Caatinga/Atlantic forest ecotone of Brazil. *CATENA, 203*, 105308.

Sari, F. (2021). Forest fire susceptibility mapping via multi-criteria decision analysis techniques for Mugla, Turkey: A comparative analysis of VIKOR and TOPSIS. *Forest Ecology and Management, 480*, 118644. https://doi.org/10.1016/j.foreco.2020.11864

Shah, S., Sen, S., & Sahoo, D. (2024). State of Indian Northwestern Himalayan lakes under human and climate impacts: A review. *Ecological Indicators, 160*, 111858. https://doi.org/10.1016/j.ecolind.2024.111858

Silva, R. M., Lopes, A. G., & Santos, C. A. G. (2023b). Deforestation and fires in the Brazilian Amazon from 2001 to 2020: Impacts on rainfall variability and land surface temperature. *Journal of Environmental Management, 326*, 116664.

Slebi-Acevedo, C. J., Silva-Rojas, I. M., Lastra-Gonzalez, P., Pascual-Munoz, P., & Castro-Fresno, D. (2020). Multiple-response optimization of open graded friction course reinforced with fibers through CRITIC-WASPAS based on Taguchi methodology. *Construction and Building Materials, 233*, 117274. https://doi.org/10.1016/j.conbuildmat.2019.117274

Sudhakar Reddy, C., Jha, C. S., Dadhwal, V. K., Hari Krishna, P., Vazeed Pasha, S., Satish, K. V., Dutta, K., Saranya, K. R. L., Rakesh, F., Rajashekar, G., & Diwakar, P. G. (2016). Quantification and monitoring of deforestation in India over eight decades (1930–2013). *Biodiversity and Conservation, 25*(1), 93–116. https://doi.org/10.1007/s10531-015-1033-2

Tzeng, G. H., & Huang, J. J. (2011). Multiple attribute decision making: Methods and applications. *Multiple Attribute Decision Making: Methods and Applications*, 1–333. CRC Press.

Vese, M., Mishra, P., Singh, W. R., Lowang, P., Assumi, S., Bandyopadhyay, A., & Bhadra, A. (2023). Decadal Variations in Area under Different Soil Erosion Classes using RUSLE and GIS: Case Studies of River Basins from Western and Eastern Arunachal Pradesh. *Journal of the Geological Society of India, 99*, 1725–1737. https://doi.org/10.1007/s12594-023-2528-1

Wagner, M., Wentz, E. A., & Stuhlmacher, M. (2022). Quantifying oil palm expansion in Southeast Asia from 2000 to 2015: A data fusion approach. *Journal of Land Use Science, 17*(1), 26–46. https://doi.org/10.1080/1747423X.2021.2020918

Wang, C. N., Kao, J. C., Wang, Y. H., Nguyen, V. T., Nguyen, V. T., & Husain, S. T. (2021). A multicriteria decision-making model for the selection of suitable renewable energy sources. *Mathematics, 9*(12), 1318. https://doi.org/10.3390/math9121318

Wilcoxon, F. (1949). *Some Rapid Approximate Statistical Procedures*. American Cyanamid Company. Stamford Research Laboratories.

Zavadskas, E. K., Turskis, Z., Antucheviciene, J., & Zakarevicius, A. (2012). Optimization of weighted aggregated sum product assessment. *Elektronika Ir Elektrotechnika, 122*(6), 3–6. https://doi.org/10.5755/j01.eee.122.6.1810

Zerouali, B., Santos, C. A. G., Do Nascimento, T. V. M., & Silva, R. M. (2023). A cloud-integrated GIS for forest cover loss and land use change monitoring using statistical methods and geospatial technology over northern Algeria. *Journal of Environmental Management, 341*, 118029. https://doi.org/10.1016/j.jenvman.2023.118029

Publisher's Note Springer Nature remains neutral with regard to jurisdictional claims in published maps and institutional affiliations.

Springer Nature or its licensor (e.g. a society or other partner) holds exclusive rights to this article under a publishing agreement with the author(s) or other rightsholder(s); author self-archiving of the accepted manuscript version of this article is solely governed by the terms of such publishing agreement and applicable law.